VARIABLE-RATE, VARIABLE-PRESSURE PRODUCTION FROM A
FRACTURED GAS WELL WITH LARGE VISCOSITY AND
COMPRESSIBILITY VARIATION: APPLICABILITY OF SUPERPOSITION
TIME

A THESIS SUBMITTED TO
THE GRADUATE SCHOOL OF NATURAL AND APPLIED SCIENCES
OF
MIDDLE EAST TECHNICAL UNIVERSITY

BY

KIYMET GİZEM GÜL ERTUNÇ

IN PARTIAL FULFILLMENT OF THE REQUIREMENTS
FOR
THE DEGREE OF DOCTOR OF PHILOSOPHY
IN
PETROLEUM AND NATURAL GAS ENGINEERING

SEPTEMBER 2017

Approval of the thesis:

VARIABLE-RATE, VARIABLE-PRESSURE PRODUCTION FROM A FRACTURED GAS WELL WITH LARGE VISCOSITY AND COMPRESSIBILITY VARIATION: APPLICABILITY OF SUPERPOSITION TIME

submitted by **KIYMET GİZEM GÜL ERTUNÇ** in partial fulfillment of the requirements for the degree of **Doctor of Philosophy in Petroleum and Natural Gas Engineering Department, Middle East Technical University** by,

Prof. Dr. Gülbin Dural Ünver
Dean, Graduate School of **Natural and Applied Sciences**   _____

Prof. Dr. Serhat Akın
Head of Department, **Petroleum and Natural Gas Engineering**   _____

Prof. Dr. Mustafa Verşan Kök
Supervisor, **Petroleum and Natural Gas Engineering Dept., METU**   _____

Prof. Dr. Erdal Özkan
Co-Supervisor, **Petroleum Engineering Dept., Colorado School of Mines**   _____

Examining Committee Members

Prof. Dr. Nurkan Karahanoğlu
Geological Engineering Dept., METU   _____

Prof. Dr. Mustafa Verşan Kök
Petroleum and Natural Gas Engineering Dept., METU   _____

Assoc. Prof. Çağlar Sınayuç
Petroleum and Natural Gas Engineering Dept., METU   _____

Assoc. Prof. Ömer İnanç Türeyen
Petroleum and Natural Gas Engineering Dept., Istanbul Technical University   _____

Asst. Prof. Tuna Eren
Petroleum and Natural Gas Engineering Dept., Batman University   _____

Date: 08/09/2017

I hereby declare that all information in this document has been obtained and presented in accordance with academic rules and ethical conduct. I also declare that, as required by these rules and conduct, I have fully cited and referenced all material and results that are not original to this work.

Name, Last name   : Kıymet Gizem Gül Ertunç

Signature   :

ABSTRACT

VARIABLE-RATE, VARIABLE-PRESSURE PRODUCTION FROM A FRACTURED GAS WELL WITH LARGE VISCOSITY AND COMPRESSIBILITY VARIATION: APPLICABILITY OF SUPERPOSITION TIME

Gül Ertunç, Kıymet Gizem

Ph. D., Department of Petroleum and Natural Gas Engineering

Supervisor   : Prof. Dr. Mustafa Verşan Kök

Co-Supervisor: Prof. Dr. Erdal Özkan

September 2017, 85 pages

The conventional approach to model gas flow in reservoirs is to use a pseudopressure transformation and assume that the remaining nonlinearity of the diffusion equation can be ignored by the weak-dependence of compressibility and viscosity on pseudopressure. However, the nonlinearity of the diffusion equation cannot be ignored in the analysis of fractured, tight-gas well performances. The nonlinearity makes the application of superposition principal questionable for fractured tight-gas well performances. Fractured, tight-gas wells produce under large pressure drawdowns, which may cause three- to ten-fold variations in the gas compressibility-viscosity product, particularly in the vicinity of the fracture, over the life of production. Not accounting for the effect of large gas compressibility-viscosity product variations in pressure- and rate-transient analysis of fractured, tight-gas well performances leads to lower permeability estimates or, in general, misinterpretation of reservoir characteristics or misassessment of the efficiency of completions.

In this research, a perturbation-Green's function solution is developed for the nonlinear gas diffusion equation. Because each term of the perturbation solution represents the solution for a linearized problem, term-by-term application of the superposition principle is permitted. The semi-analytical nature of the solution also enables us to

derive approximations for practical use. This dissertation explains the solution procedure, compares and verifies the solution by a spectral solution and by a numerical simulator, presents variable-rate approximations in terms of a new superposition time, and discusses the results to provide guidelines for the analysis of fractured, tight-gas well performances under large variations of viscosity and compressibility.

Keywords: perturbation method, Green's function, superposition time, pseudopressure, tight-gas well performance, gas production

ÖZ

YÜKSEK AKMAZLIK VE SIKIŞTIRILABİLİRLİK DEĞİŞİMİ OLAN ÇATLAKLI GAZ KUYUSUNDAN DEĞİŞKEN DEBİLİ VE DEĞİŞKEN BASINÇLI ÜRETİM: ZAMANDA SÜPERPOZİSYON UYGULANABİLİRLİĞİ

Gül Ertunç, Kıymet Gizem

Doktora, Petrol ve Doğal Gaz Mühendisliği Bölümü

Tez Yöneticisi   : Prof. Dr. Mustafa Verşan Kök

Ortak Tez Yöneticisi: Prof. Dr. Erdal Özkan

Eylül 2017, 85 sayfa

Rezervuarlarda gaz akışının modellemesine yönelik klasik yaklaşım, yalancı-basınç tanımını kullanarak, sıkıştırılabilirliğin ve akmazlığın yalancı-basınç ile zayıf bağımlılığı olduğunu varsayıp difüzyon denkleminin doğrusal olmayışını göz ardı etmektedir. Ancak difüzyon denkleminin doğrusal olmaması, çatlaklı, kesif gaz kuyu performansı analizlerinde göz ardı edilemez ve bu doğrusal olmayış süperpozisyon kuralının çatlaklı kesif gaz kuyu performansı analizlerinde uygulanabilirliği konusunda soru işaretleri oluşturur. Çatlaklı kesif gaz kuyuları, üretim ömrü boyunca, özellikle çatlak çevresinde, gaz sıkıştırılabilirlik katsayısı ve akmazlığı üzerinde 3-10 katı değişikliğe neden olabilecek yüksek basınç düşüşleri altında üretilirler. Gaz sıkıştırılabilirlik katsayısı ve gaz akmazlığı değişiminin kesif gaz kuyu performansında göz önüne alınmaması, geçirgenlik tahminlerinin daha düşük olmasına, genel olarak rezervuar özelliklerinin yanlış yorumlanmasına veya kuyu tamamlama değerlendirmesinin hatalı olmasına neden olur.

Bu araştırmada, doğrusal olmayan gaz difüzyon denklemi için pertürbasyon-Green fonksiyonu çözümü geliştirilmiştir. Pertürbasyon çözümünde, çözümünün her bir

terimi, doğrusal bir sorunun çözümünü temsil ettiğinden, süperpozisyon ilkesinin adım adım uygulamasına izin vermektedir. Çözümün yarı analitik yapısı da pratik kullanım için yaklaşımlar türetmeye olanak sağlar. Bu tezde sunulan çözüm, spectral çözüm ve numerik simülatör ile karşılaştırıldı ve doğrulandı. Çözüm prosedürü, değişken debili yaklaşımları yeni bir süperpozisyon zamanı ile sunar, viskozite ve gaz sıkıştırılabilirlik katsayısındaki yüksek değişimlerin çatlaklı kesif gaz kuyusu performansına etkisinin analizlerini tartışır.

Anahtar kelimeler: pertürbasyon metodu, Green fonksiyon, superpozisyon zamanı, yalancı-basınç, kesif kuyu performansı, gaz üretimi

to my family

ACKNOWLEDGEMENTS

TABLE OF CONTENTS

LIST OF FIGURES

FIGURES

LIST OF TABLES

NOMENCLATURE

c_g	Gas compressibility, psia^{-1}
c_{gi}	Initial gas compressibility, psia^{-1}
c_t	Total compressibility, psia^{-1}
c_{ti}	Initial total compressibility, psia^{-1}
$E_i(x)$	Constant (unit) rate pressure response, psi
$erfc(x)$	Complementary error function
G	Green's function
h	Fracture height, ft
k	Permeability, mD
$m(P)$	Real gas pseudopressure/Real gas potential, psia^2/cp
N_p	Cumulative oil production, STB
P	Pressure, psia
P'	Dummy pressure integration variable, psia
P_i	Initial pressure, psia
P_b	Base pressure, psi
P_{pc}	Pseudo-critical pressure, psi
P_{pn}	Normalized pseudopressure, psi
$P_u(t)$	Constant (unit) rate pressure response, psi
q_g	Gas flow rate, Mscf/day
q_o	Oil flow rate, STB/day
T	Reservoir temperature, R
T_{pc}	Pseudo-critical temperature, R
t	Flowing time, day
t'	Dummy time variable

t_a	Real gas pseudo-time, hr-psi/cp
$\bar{t}$	Material balance time, days
$\overline{t_a}$	Normalized material balance pseudo-time, days
t_{pn}	Normalized pseudo-time, hr
t_n	Normalized pseudo-time, days
x_f	Fracture half-length, ft
y'	Dummy y-axis integration variable
z	Gas deviation factor

Greek Symbols

ε	Perturbation term
ϕ	Porosity, fraction
η	Hydraulic diffusivity
μ	Viscosity, cp
μ_g	Viscosity of gas, cp
μ_{gi}	Initial gas viscosity, cp
ρ_g	Gas density, lbm/ft^3
τ	Dummy variable
Δ	Difference operator
∇	Spatial derivative operator
ω	Diffusivity gas deviation factor

CHAPTER 1

INTRODUCTION

The main objective is to provide an analytical solution to investigate the effect of pressure-dependent viscosity-compressibility product on the performances of hydraulically fractured, tight-gas wells and provide guidelines to improve the analysis and interpretation of pressure and production data. This problem becomes prevalent particularly in tight, unconventional-gas reservoirs where large pressure gradients are required to produce the gas causing significant (up to three to ten folds) variations of gas viscosity and compressibility during production.

Under Darcy-flow conditions, flow of fluids in porous media are governed by the diffusion equation. For the flow of a real gas, pressure-dependent fluid properties make the diffusion equation nonlinear that require approximate numerical or analytical techniques for solution. For the numerical simulation of real-gas flow problems, severe variations of viscosity and compressibility impose time-step restrictions to ensure numerical stability and accuracy. For analytical solutions, the first resort is to apply a transformation to linearize the diffusion equation. The pseudopressure, $m(P)$, transformation introduced by Al-Hussainy et al. [1] has been the most common of these transformations. However, the pseudopressure transformation leaves some nonlinearity in the diffusion equation, which may be ignored if the variation of fluid properties is not expected to be significant during the period of analysis (e.g., short-duration pressure transient tests). In other cases, appropriate solution approaches have to be adopted to effectively deal with the nonlinearity of the problem while retaining the practicality of the solution.

1

Recently, Barreto et al. [2] [3] proposed a perturbation-Green's function solution by using the change in the viscosity-compressibility as a source term. This approach is promising to develop a semi-analytical solution for the problem under consideration in this dissertation. The particular emphasis in this work is to extend the approach proposed by Barreto et al. [2] [3] to computationally more efficient forms which enhances the practical utility of the solution as well enabling derivation of approximate forms for practical data analysis.

Perhaps, the most salient feature of the perturbation-Green's function solution is its potential to use with the superposition principle despite the nonlinearity of the underlying problem. Superposition principle is commonly used in petroleum engineering to develop solutions for complex boundary conditions, such as variable-rate production or no-flow boundaries, by using the solutions for constant-rate production and infinite-acting reservoir. However, the nonlinearity of the gas diffusion equation prevents the application of the superposition principle in gas flow problems. Using the perturbation approach, the nonlinear problem is replaced by a series of linear problems, which permits the term-by-term application of the superposition principle.

1.1. Dissertation Organization

This dissertation consists of six chapters, in the following organizational structure:

Chapter I provides an introduction of the research topic and description of the research objectives, motivations, contributions and significance of the research.

Chapter II presents a literature review and discusses the background of the developments and discussions in the following sections.

Chapter III provides the details of the problem formulation and solution together with the verifications of the solution.

In Chapter IV, practical approximations are given, derivation of a superposition time for data analysis is presented, and extensions to other physical problems are discussed.

Chapter V presents a discussion of the results and example applications to practical problems of interest.

Chapter VI, provides a summary of the accomplishments and conclusions of this work and makes recommendations for future studies.

1.2. Research Problem

Most fractured tight-gas well performance data are available under the condition of variable production rate. If the conditions of flow grant the assumption of a linear diffusion equation, variable-rate production solutions can be obtained by the superposition of constant-rate solutions. Solutions developed by this approach enable the extension of the standard analysis techniques developed for the constant-rate problem to variable-rate production data by using relatively simple modifications, such as the definition of a superposition time. Severe variations of gas viscosity and compressibility in tight-gas fields, however, impose a strong nonlinearity on the diffusion equation, which cannot be removed by the standard pseudopressure transformation. Consequently, relatively simple, closed-form analytical solutions cannot be obtained by the conventional approaches. Available approximate analytical and numerical solution options for these cases usually encounter efficiency and accuracy problems due to computational limitations and, most importantly, they are not amenable to the use of superposition to obtain variable-rate solutions. This dissertation undertakes the challenge to develop a perturbation-Green's function solution for fractured tight-gas well performances under strong variations of gas viscosity and compressibility, which can be used to analyze variable-rate and variable-pressure production data.

1.3. Research Objectives

The main objective of this dissertation is to express flow toward a fractured well in a tight-gas reservoir with strong variability of gas viscosity and compressibility in the form of a perturbation problem and obtain an approximate analytical solution in terms of a series of Green's function solutions to a set of linear problems, which permits term-by-term term application of the superposition principle. This research has been inspired by the perturbation-Green's function approach proposed by Barreto et al. [2] [3] for the solution of nonlinear diffusion equation and is a continuation of the MSc thesis research of Komurcu [4].

The specific objectives of the research are the following:

- Extend the approach proposed by Barreto et al. [2] [3] to computationally more efficient forms which enhances the utility of the solution;
- Derive mathematically coherent approximate forms of the solution for practical data analysis;
- Develop a superposition time for practical data analysis based on the approximate solution;
- Discuss the extensions of the solution to other physical problems of interest;
- Present example applications to demonstrate the utility of the solution;
- Provide guidelines for the analysis and interpretation of fractured well performances in tight-gas reservoirs under strong variability of gas viscosity and compressibility.

1.4. Motivation, Contribution, Significance

Multi-fractured tight-gas wells have been the driver behind the shale-gas revolution in the last two decades. Numerical, analytical, and empirical methods have been used to

analyze and predict the performances of wells in tight-gas reservoirs. Numerical methods (mainly commercial simulators) are employed to deal with the complexities, such as extreme geologic heterogeneity, multi-phase flow, and nonlinearity of the problem if sufficient data and computational resources are available. An approximate solution is obtained from numerical methods where the success of simulations is controlled by grid and time-step requirements and the accuracy is improved at the expense of onerous computational efforts.

On the other hand, empirical methods, such as decline curve analysis and, to some degree, brute force application of data analytics, have their utility in situations where minimal data (usually only the well-head production) are acquired and limited resources are afforded for the analysis. Despite their wide-spread use in reserve estimations and economic investment decisions, however, the roots of the empirical methods (mostly based on the observations from vertical wells in conventional reservoirs) raise skepticism on their application to fractured tight-gas wells and the lack of a solid physical basis further lowers the trust in them.

Between the two ends (large data and computational-resource needs of numerical simulation and oversimplification inherent in the empirical techniques), analytical tools offer a compromise, which is appreciated at least for initial investigations, and a physical understanding, which can guide both numerical simulation studies and empirical interpretations. Closed-form solutions resulting from analytical methods are also useful to determine the functional dependencies of the well performances on the physical and well-completion parameters involved. However, the use of fully analytical methods requires certain mathematical conditions; linearity of the problem being one of the requirements. To this end, the nonlinearity of the real-gas flow equation has always been one of the most fundamental limitations for fully analytical solutions. Linearization of the gas-diffusion equation by pseudopressure transformation of Al-Hussainy et al. [1] does not provide an adequate practical solution when the viscosity-compressibility product becomes a strong function of pressure, which is the most common condition in tight, unconventional gas fields.

5

A related problem is the treatment of variable-pressure- and variable-rate-production conditions, which is traditionally handled by the superposition of constant-rate-production solutions. However, the condition of linearity makes the superposition approach inapplicable for tight-gas wells, where most data are obtained under variable-pressure- and variable-rate-production conditions. Therefore, a useful feature of any solution for tight-gas wells is to be amenable for superposition.

When fully analytical solutions are not permitted by the physical conditions of the problem, an alternate option is to resort to semi-analytical techniques. Therefore, one of the motivations of this research is to provide semi-analytical tools for performance predictions and data analysis of tight-gas wells. The method of perturbations is one of the most common semi-analytical approaches to find approximate analytical solutions to nonlinear partial differential equations. Recently, Barreto et al. [2] [3] proposed to combine perturbation and Green's function approaches to solve the nonlinear diffusion equation. They considered the nonlinearity of the diffusion equation due to strong pressure-dependence of viscosity and compressibility product and showed that adding the first order perturbation to the solution of the linear problem creates sufficiently accurate results for most practical purposes. They also suggested extensions of the perturbation-Green's function solution to non-Darcy flow and variable-rate production by superposition, but they did not demonstrate these applications (except for the case of pressure buildup problem).

Barreto et al. [2] [3] presented the basis of their approach and provided the verification of their solution. However, their solution requires numerical evaluation of convolution integrals, which is highly unstable and computationally intensive. Later, Ahmadi [5], Komurcu [4] and Bila [6] used the same approach to derive approximate analytical solutions for tight (1D fractured gas well) and high-permeability (non-Darcy flow) reservoirs, respectively, but they did not arrive at convincingly accurate and practical solutions.

6

The works of Barreto et al. [2] [3] have provided the inspiration for this research to derive a practical solution for fractured tight-gas wells under high variability of viscosity and compressibility. Unlike the solution of Barreto et al. [2] [3], which requires numerical integration of convolution integrals, this work discretizes and analytically solves the integrals appearing in the solution. This additional analytical treatment leads to computationally more efficient forms of the solution, which enables identification of parametric relationships, physically more sound approximations, and derivation of superposition-time functions. With the new features of the solution, it becomes possible to identify the conventional flow regimes on variable-rate- and variable-pressure data of fractured tight-gas wells and analyze the data by the conventional approaches. Moreover, the improved form of the solution enables easier extensions to other problems, such as stress dependent permeability in unconventional reservoirs.

1.5. Assumptions and Hypotheses

The derivation of the solution presented in this work involves the following assumptions:

- Homogeneous formation of constant thickness
- Infinite-acting reservoir
- Uniform permeability, and porosity
- Darcy flow
- Permeability independent of pressure (unless specified otherwise)
- Formation saturated with a homogeneous fluid (gas)
- Isothermal gas flow
- No gravity
- No compositional changes
- 1D linear flow toward an infinite-conductivity fracture
- Fully penetrating fracture
- Uniform flux along the length and height of the fracture

Under these conditions, the main hypothesis of the research is that a perturbation-Green's function solution can be derived for the 1D, linear flow of a real gas toward a fractured well in an infinite, homogeneous reservoir. The solution permits extensions to variable-rate problems by the application of superposition principle.

CHAPTER 2

LITERATURE REVIEW AND BACKGROUND

This chapter presents a review of literature for variable rate problems and solutions to nonlinear gas flow problems. Modelling of gas flow is complicated because of the nonlinearity of the gas diffusion equation. Variable-rate problems can be handled by superposition principle for slightly compressible fluids; however, for compressible fluids superposition does not work since the linearity requirement does not satisfied. A comprehensive review was performed for the variable rate and nonlinear problems in this chapter. Solutions were categorized under relevant topics.

2.1. Equation of Gas Flow through Porous Media

The governing equation for the flow of gas through porous media is the diffusivity equation. The diffusion equation for the real gas flow through porous media is;

$$\overline{\nabla}\left[\frac{P}{\mu_g(P)z(P)}\overline{\nabla}P\right] = \frac{\mu_g(P)\phi c_t(P)}{k}\frac{P}{\mu_g(P)z(P)}\frac{\partial P}{\partial t} \qquad (2.1)$$

Diffusivity term is defined as;

$$\eta = \frac{k}{\mu_g(P)\phi c_t(P)} \qquad (2.2)$$

The Equation (2.1) is nonlinear because the fluid properties such as viscosity, gas deviation factor and gas compressibility are functions of pressure. Unlike slightly

compressible fluids (such as oil), removing the nonlinearity from the real gas diffusion equation by physically acceptable assumptions is not possible.

Formerly, the usual approach is to use the same diffusivity equation for gas and oil flow but the difference is to use the pressure for oil flow and pressure-squared for gas flow [7]. It was proved that at high pressures to use P instead of P^2 was also appropriate for gas reservoirs [8]. Later, Al-Hussainy et al. [1] introduced a third variable known as pseudopressure or real gas potential, $m(P)$. Since pseudopressure approach contains the least number of assumptions in terms of gas diffusion equation, it can be considered as the most accurate one from all above the three for pressure transient analysis gas wells (P, P^2, $m(P)$) [9]. Pseudopressure approach groups the pressure and pressure dependent properties into a new variable and aims to form a gas diffusion equation in which the nonlinearity is weaker. Pseudopressure is defined as;

$$m(P) = 2\int_{P_b}^{P} \frac{P'}{\mu(P)z(P)} dP'$$

(2.3)

With the use of pseudopressure, a second order, nonlinear partial differential equation with variable coefficients is obtained as follows for the gas flow through porous media;

$$\nabla^2 m(P) = \frac{\phi\mu_g(P)c_t(P)}{k} \frac{\partial m(P)}{\partial t}$$

(2.4)

The original implementation of the pseudopressure approach is at low flow rates, at high pressures or when the pressure change is small through the application as in the case of gas well test data or transient flow periods during which the reservoir pressure does not significantly deviate from the initial pressure. Under these conditions, variation of viscosity-compressibility product with pressure can be neglected.

Even with the use of pseudopressure approach accounting for the variation of viscosity and gas deviation factor with pressure, Equation (2.4) is still nonlinear because of the

existence of viscosity and gas compressibility which are also dependent on pressure. When transient flow lasts long to cause considerable pressure drop as in the fractured unconventional reservoirs or when there is a steep pressure decline as in the boundary dominated flow, the constant viscosity-compressibility assumption is not valid [10]. As a consequence, true pseudo-steady state is not observed in gas wells which makes applicability of the standard gas well performance prediction techniques questionable.

It is evident from Figure 2.1 and Figure 2.2 that there is a steep change in both viscosity-compressibility product and relative change of viscosity-compressibility product at low pressures; however, they become almost constant when the pressure approaches to initial reservoir pressure. That means that viscosity-compressibility product is clearly a function of pseudopressure.
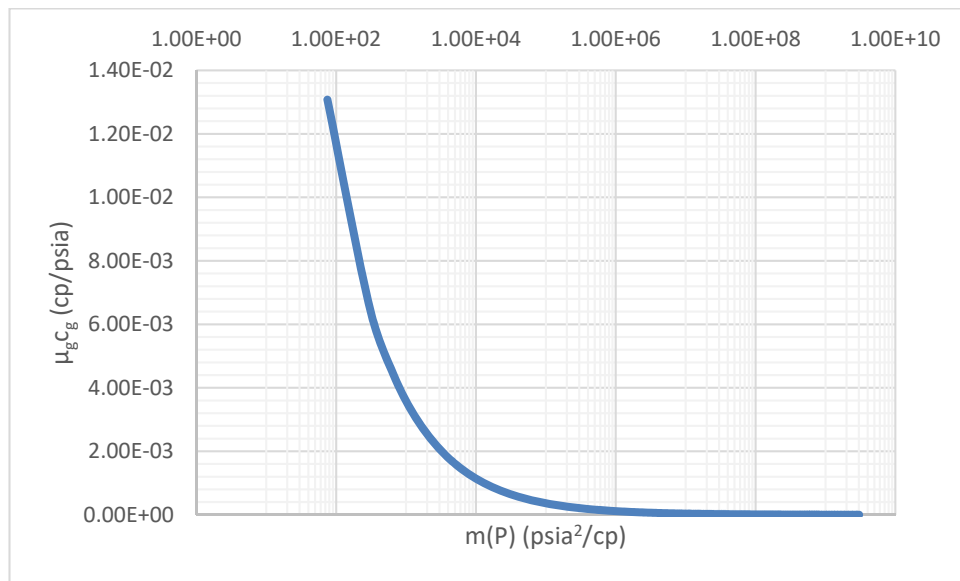
Figure 2.1. Variation of viscosity-compressibility product with pseudopressure
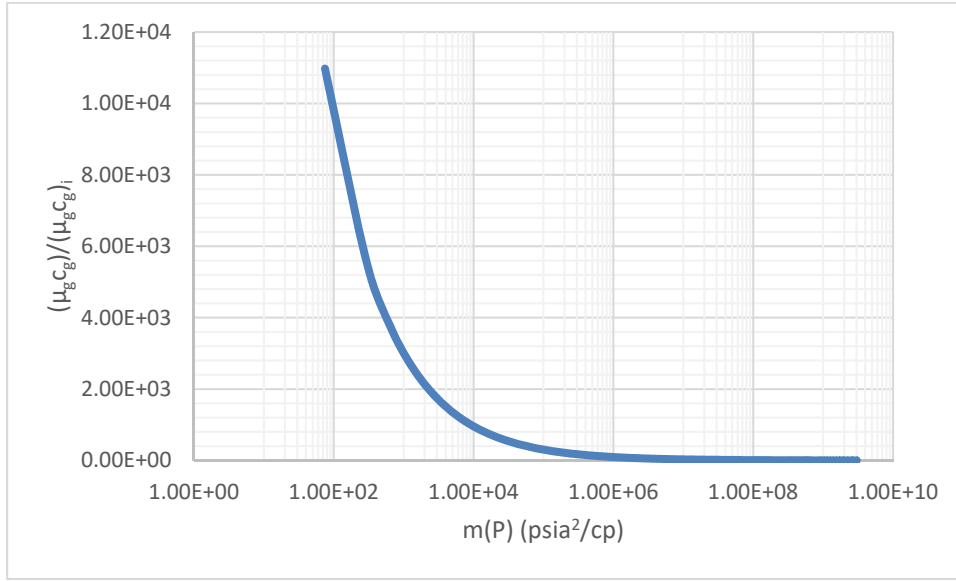
Figure 2.2. Relative change of viscosity-compressibility product with pseudopressure

To remove the nonlinearity, Agarwal [11] introduced a new transformation, known as real gas pseudo-time, t_a, is given by;

$$t_a(t) = \int_0^t \frac{1}{\mu(t')c_t(t')} dt'$$ (2.5)

This transformation takes into account the variation of gas viscosity and compressibility with pressure, and correspondingly as a function of time. Fluid properties are evaluated at wellbore pressure. Finjord [12] proved that pseudo-time transformation does not linearize the early drawdown data during transient flow period. Lee and Holditch [13] confirmed that use of pseudo-time approach with pseudopressure effectively linearize gas diffusion equation.

Palacio and Blasingame [14] introduced material balance pseudo-time for liquid flow as follows;

$$\bar{t} = \frac{N_p}{q_o(t)}$$ (2.6)

and material balance pseudo-time for gas flow;

$$\overline{t_a} = \frac{\left(\mu_g c_t\right)_i}{q_g} \int_0^t \frac{q_g}{\mu_g\left(\overline{P}\right)c_t\left(\overline{P}\right)} dt \qquad (2.7)$$

Material balance pseudo-time function allows to model single phase flow by using Fetkovich liquid type curve at slightly changing bottomhole pressure conditions. Later, Agarwal et al. [15] proved that material balance pseudo-time converts constant pressure solution into constant rate solution which is the primary goal for well test analysis. This definition requires the use of average reservoir pressure to estimate the fluid properties in order to calculate material balance pseudo-time. In order to estimate average reservoir pressure, original gas in place knowledge is required which requires an iterative procedure.

Fraim and Wattenbarger [16] developed real gas normalized time definition to consider the variation of gas properties;

$$t_n = \int_0^t \frac{\left(\mu c_t\right)_i}{\mu\left(\overline{P}\right)c_t\left(\overline{P}\right)} dt \qquad (2.8)$$

The normalized time is developed for gas wells producing under constant wellbore pressure condition during boundary dominated flow in closed reservoirs. According to this method, fluid properties are calculated at average reservoir pressure. The purpose is to use Fetkovich type curve for gas wells.

Meunier et al. [17] introduced normalizations to pseudopressure and pseudo-time definitions. Al-Hussainy et al. [1] pseudopressure definition is normalized as follows;

$$P_{pn} = 2\frac{\mu_i z_i}{P_i} \int_{P_b}^{P} \frac{P}{\mu(P)z(P)} dP \qquad (2.9)$$

and Agarwal [11] pseudo-time normalized as follows;

$$t_{pn} = \mu_i c_i \int_0^t \frac{1}{\mu(P)c_t(P)} dt$$

(2.10)

The use of normalized pseudopressure and normalized pseudo-time transformation together results in retaining of units of pressure and time (unlike psi^2/cp, it has unit of pressure) for both gas and liquid cases. It allows the use of same constants for liquid and gas flow equation.

Ibrahim et al. [18] proposed new normalized pseudo-time approach;

$$t_n = (\phi\mu c_t)_i \int \frac{1}{\phi(\overline{p})\mu(\overline{p})c_t(\overline{p})} dt$$

(2.11)

Normalized pseudo-time function is used in the superposition time method for smoothing the production field data. The use of this method takes into account the change in reservoir properties with average reservoir pressure and more accurately calculates original gas in place. It gives satisfactory results for the production data analysis in highly depleted reservoirs with high compressibility. The new normalized pseudo-time can be used for the variable rate and variable pressure gas well performance prediction.

2.2. Superposition Principal

The superposition principle states that, for all linear systems, the response of the total system at a given point or time is sum of the responses of each individual stimulus. Superposition principle is a mathematical technique used in petroleum engineering to solve more complex boundary conditions such as variable rate and bounded reservoirs by using the simpler solutions developed for constant rate and infinite-acting

14

reservoirs. Superposition in space, also known as method of images, is used to construct solutions for more complex well geometries, bounded reservoirs and multiple well problems. Superposition in time is used to construct solutions for variable rate and pressure buildup. Superposition technique is only applicable for linear systems. If nonlinearities appear in the equation (e.g. gas flow) to apply superposition, linearization techniques (e.g. pseudopressure transform) must be performed.

Convolution is a mathematical operation between two functions $f(t)$ and $g(t)$ producing a third function $\psi(t)$ which represent the overlap amount between $f(t)$ and the reversed or shifted function of $g(t)$. The convolution between two functions $f(t)$ and $g(t)$ can be written in mathematical form as;

$$
\begin{aligned}
\psi(t) = f(t) * g(t) &= \int_0^t f(\tau)g(t-\tau)d\tau \\
&= g(t) * f(t) = \int_0^t f(t-\tau)g(\tau)d\tau
\end{aligned}
\tag{2.12}
$$

The discrete form of the Equation (2.12) over a finite domain can be written as;

$$
\psi(t) \approx \sum_{i=1}^n f(\tau_{i-1})g(t-\tau_{i-1})\Delta\tau_i
\tag{2.13}
$$

where τ is the dummy variable, $\psi(t)$ is the system response, $f(t)$ and $g(t)$ are the convolution functions. The convolution or superposition equation indicates that the total response of the system is equal to the summation of each individual stimulus.

In regards to petroleum engineering, the superposition principal can be applied to linear diffusivity equation in which there is a linear relationship between pressure and flow rate. If the linearity requirement is satisfied, the total pressure response of the reservoir under variable rate condition is equal to the summation of individual pressure

15

responses of each rate change since the time of each rate change. Duhamel's principal states that the pressure drop for the variable rate system is equal to the convolution of the input rate function and the derivative of the impulse function or the derivative of constant rate pressure response. The system is assumed to be equilibrium at $t=0$ (i.e. $P(x,t=0)=P_i$).The convolution (Duhamel's/superposition) integral is defined as;

$$\Delta P(t) = \int_0^t q(t-\tau)P_u'(\tau)d\tau \tag{2.14}$$

The discrete form of the Equation (2.14);

$$\Delta P(t) = \sum_{i=1}^n (q_i - q_{i-1})P_u(t-t_{i-1}) \tag{2.15}$$

The Duhamel's principal was introduced to the literature with van Everdingen and Hurst [19] to obtain a dimensionless wellbore pressure drop response solution for a continuously (smoothly) varying rate production. They convolved the smooth rate profile with constant rate pressure response in order to get the variable rate pressure drop response. Odeh and Jones [20] used semi-log approximation whereas Soliman [21] used exponential integral approximation of constant rate wellbore pressure response function in order to evaluate variable pressure data. van Everdingen and Meyer [22] applied the superposition approach to low permeability, vertical fractured wells in order to analyze pressure buildup data. They proved that Odeh and Jones method does not give reasonable results for the interpretation of buildup data in low permeability reservoirs. They apply superposition to dimensionless vertical fracture constant rate solution. In order to find a relation between dimensionless time and real time, they proposed a trial and error procedure with the initial estimate provided by conventional Horner analysis. Fetkovich and Vionet [23] modified the Odeh and Jones method and include dimensionless pressure approximation instead of log approximation. They derived plotting functions for a uniform flux vertical fractured well by using constant rate flow equation. These plotting functions are not valid for

boundary effected flow tests. Bostic et al. [24] employed the superposition to calculate a unit function. This unit function is a transformation to the equivalent pressure history with constant rate of well/reservoir system that has produced a variable rate with a known pressure history. This approach is similar to the van Everdingen and Hurst [19] approach for aquifers and to Jargon and van Poollen [25] for variable rate, variable pressure well tests. Agarwal [26] introduced a new method for correction of buildup data from producing time effects for variable rates by using Duhamel's principal.

Cinco-Ley and Samaniego [27] presented the advantages and limitations of using superposition time concept to several flow regimes during pressure buildup tests. Samaniego and Cinco-Ley [28] took into consideration the effect of high velocity flow and damage in variable rate gas wells. Their method, applicable to infinite acting radial flow gas reservoirs, develops a step-function approximation to flow rate to account for the small changes in pressure and the gas properties taken at initial conditions. It can be applied to discretized continuously varying flow rate tests. Gupta and Andsager [29] described the pressure behavior of gas well with superposition principal and Horner's point source solution of radial diffusivity equation. According to their method, viscosity and z-factor is calculated at average reservoir pressure and diffusivity term was assumed to be constant. von Schroeter and Gringarten [30] applied superposition principle to nonlinear problems; however, they also assumed the diffusivity term as constant.

2.3. Rate Normalization

The rate normalization method was first introduced by Gladfelter et al. [31] to use both pressure and downhole flow rate data for the wellbore storage correction in gas well pressure buildup analysis. They claimed that pressure rise after shut-in divided by instantaneous change in downhole flow rate is a linear function of logarithm of production time. It is actually the substitute of conventional superposition. Ramey [32] confirmed the validity of Gladfelter et al. [31] correction for buildup case and the use of this approach for short time gas well drawdown data except for non-Darcy flow

17

effects. Kuchuk [33] showed that the Gladfalter [31] deconvolution is only valid for only few simple geometries and for linearly varying flow rates.

Winestock and Colpitts [34] employed rate normalization to drawdown data of gas wells and obtained straight line in semi-log plot. They proposed is valid if flow rate changes smoothly even though the total flow rate change is large. Their method did not have any application for wellbore storage distorted data; however, it can be used to correlate constant rate analysis for constant pressure condition.

Odeh and Jones [20] developed an iterative procedure for both oil and gas wells flowing at variable rates. They used the logarithmic approximation for exponential integral solution at each constant rate steps.

Fetkovich and Vienot [23] applied Gladfelter approach to a hydraulically fractured oil well at initial completion. In order to identify boundaries, linear flow permeability changes near to wellbore, accurate pressure and total afterflow fluid rate measurements are required for a reservoir whose early time data is affected from wellbore storage.

Earlier studies of Gladfelter et al. [31], Winestock and Colpitts [34], Odeh and Jones [20], among others have advocated to measuring the downhole flow rate and analyzing well tests by variable rate test methods. However, the use of production logging tools for the simultaneous transmission of rate and pressure was first conducted by Meunier et al. [35]. Using measured sandface rate data, Meunier et al. [35] introduced rate convolved buildup time function in order to modify Horner time ratio. They showed that using rate convolved buildup time function reduces the time to reach the semi-log straight line prior to 1½ log cycle rule or type curves.

Kuchuk and Ayestaran [36] developed a Laplace transform based method to calculate formation pressure from the deconvolution of sandface flow rate and measured wellbore pressure data without wellbore storage effects. Formation parameters, wellbore and reservoir geometries can be estimated from this calculated formation

pressure. However, this method's drawbacks are calculation of only constant unit rate pressure drop and fluctuation of its logarithmic derivative [37].

When both bottomhole pressure and sandface flow rate data are available, Thompson and Reynolds [38] considered the use of Duhamel's principal to pressure buildup and drawdown data. Duhamel's principal can be applied to convert bottomhole pressure data obtained at variable sandface flow rate to the equivalent pressure data that would have been obtained at constant sandface flow rate. Therefore, the standard solution techniques (type curve matching or semilog analysis) can be used with the equivalent pressure data obtained. Equivalent pressure analysis is more advantageous than rate normalization technique to use when the data are strongly affected by wellbore storage effects. However, in most cases rate normalization technique is applicable and more simple to use.

2.4. Numerical Methods

Most of the reservoir engineering equations are nonlinear partial differential equations which cannot be solved analytically easily. That is why numerical techniques must be employed to solve these differential equations. Finite difference is the most common numerical method used in petroleum engineering. In this work, Eclipse [39] was used as a finite difference simulator and Thompson's spectral solution [40] were used as a spectral method.

2.4.1. Finite Difference Method

The solution of the flow equations in reservoir engineering is actually the determination of the dependent variables on time and space. In finite difference method, the time domain is discretized into time steps during which the problem is going to be solved and dependent variables are going to be obtained. The space domain is also divided into a number of finite difference grids. In order to improve the accuracy of the solution, smaller time steps and very fine grids are required which increase the run time and round off errors. The partial differential equation is replaced by its

approximate finite difference equations. These approximate equations are obtained by truncating the Taylor's series expansion of the unknown variables as a function of a given point [41]. Truncation error due to the Taylor's expansion approximation increases numerical dispersion [42].

2.4.2. Finite Element Method

The difference between finite element method and finite difference method is that while finite element method is an approximation to the solution of the partial differential equation, finite difference method is an approximation to partial differential equation. Finite element methods discretize the problem space domain into a set of subdomains which is called finite element. The solution of the differential equation is approximated over the finite element. Noticeably, the approximated solution cannot satisfy the differential equation and remains some residue behind. This residue should be minimized by weighted residual formulation with appropriate weighting function [42].

2.4.3. Boundary Element Method

In boundary element method, the bounding surface is discretized unlike in finite element and finite difference methods, the domain is discretized i.e. boundary element method is a surface method whereas the other two is domain methods. Due to domain discretization, finite element and finite difference methods suffer from grid orientation and numerical dispersion [43]. Although boundary element methods have the accuracy of analytical methods, it is less common in oil industry [44].

2.4.4. Spectral Method

Spectral methods are used to solve any kind of differential equations numerically by approximating the solution as a sum of continuous functions (such as Fourier series which are sinusoids or Chebyshev polynomials) over the whole domain. The main difference of spectral methods and finite difference methods is that while spectral

methods approximate the solution, finite difference methods approximate the differential equation to be solved. Similar to finite element methods, spectral methods also approximate the solution. However, the big difference is in approximations for the solution domain, in finite element method approximations are in local, whereas in spectral methods the approximations are valid throughout the entire computational domain [42]. Partially for this reason, spectral methods have excellent error properties (exponential convergence) when the solution is smooth.

The accurate solutions can be obtained by spectral methods up to 30-60 terms. Similar accuracy can be obtained with finite difference with hundreds to thousand grids [45]. Incorporation of nonlinear terms (like pressure dependent permeability, fluid properties, non-Darcy flow) is easy [45].

In this research, in order to obtain accurate solutions to nonlinear gas diffusion equation, spectral method [45] is used. The solution is approximated by a backward Euler finite difference approximation in time and a truncated Chebyshev series in space. The detailed derivation and verification of Thompson's spectral solution [40] can be found in Komurcu MSc thesis [4].

2.5. Perturbation Approach (Asymptotic Expansion)

Perturbation approach is one of the common approaches to solve the nonlinear equations. It breaks the nonlinear problem into a solvable/perturbation linear parts. Perturbation technique is applicable to the problems that cannot be solved exactly. To solve small disturbances, ε are added to the exact problem.

According to the perturbation theory, an approximate solution to full solution x, in terms of power series in small parameter (ε), can be described as follows;

$$x = x^{(0)} + \varepsilon^1 x^{(1)} + \varepsilon^2 x^{(2)} + \varepsilon^3 x^{(3)} + ... = \sum_{k=0}^{\infty} \varepsilon^k x^{(k)} \tag{2.16}$$

The first term in the right hand side of the equation ($x^{(0)}$) is the solution for exactly solvable problem. The higher terms ($x^{(0)}, x^{(1)}, x^{(2)}, ...$) describes the deviation from the exact solution. $x^{(k)}$ represents the order of the solution. The solution can be obtained by taking the limit as $\varepsilon \to 0$. If ε is small and the coefficients ($x^{(0)}, x^{(1)}, ..., x^{(k)}$) are independent of ε , then;

$$x^{(0)} = x^{(1)} = x^{(2)} = ... = x^{(k)} \tag{2.17}$$

The nonlinearity in the gas diffusion equation comes from the diffusivity term. In order to remove the nonlinearity perturbative and self-similar techniques have been applied. Kale and Mattar [46] were among the first to apply perturbation theory to diffusivity term in gas flow equation and used Boltzmann self-similar variable in order to develop an approximate first order solution for constant rate radial flow. Peres et al. [47] [48] also applied perturbation solution and Boltzmann self-similar transformation to a line source well located in infinite, homogeneous gas reservoir producing with constant surface flow rate. They showed that the perturbation solution truncated in the second order perturbation gave sufficiently accurate results for engineering purposes. Unfortunately, Boltzmann transformation technique are only applicable to self-similar problems which restricts the use of them to several nonlinear well testing problems. Recently, Barreto et al . [2] [3] applied the perturbation theory to the nonlinear gas diffusivity equation by the use of Green's function. They obtained a solution of a Volterra integro-differential of the second kind which is implicit and need to be iterated. Komurcu [4] applied perturbation-Green's function solution to unconventional gas reservoirs and solved the nonlinear gas diffusion equation analytically; however, convincingly accurate results were not obtained.

CHAPTER 3

PROBLEM FORMULATION, SOLUTION, AND VERIFICATION

In this chapter, the formulation of the 1D, linear flow problem of a real gas toward a fractured well in an infinite, homogeneous reservoir is presented and converted to an expression in terms of pseudopressure. The resulting diffusion equation is expressed in the form of a perturbation problem and its solution is assumed as a perturbation series, which creates a set of linear problems for each perturbation. The solutions for the zero and first order perturbation problems are presented and the solution is verified by the existing analytical and numerical methods.

One dimensional, linear flow toward a fracture in an infinite reservoir can be schematically represented as in Figure 3.1.
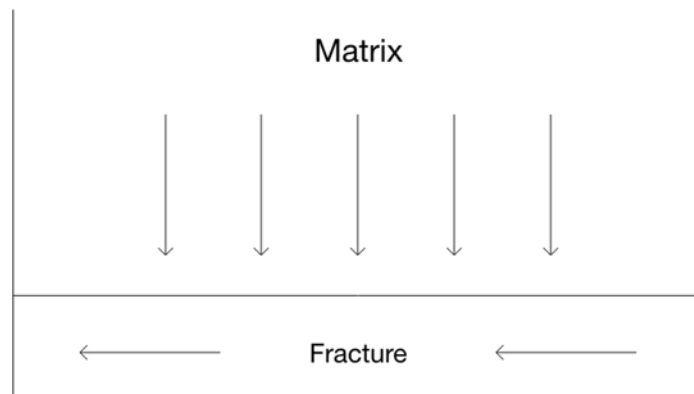
Figure 3.1. Reservoir schematics for 1D fracture flow

3.1. Mathematical Formulation of the Physical Problem

The diffusion equation for the 1D, linear flow problem of a single-phase, real gas toward a fractured well in an infinite, homogeneous reservoir is given by;

$$\frac{\partial}{\partial y}\left(\rho_g \frac{k}{\mu_g}\frac{\partial P}{\partial y}\right) = \frac{\phi \rho_g c_t}{6.328\times10^{-3}}\frac{\partial P}{\partial t} \tag{3.1}$$

with the initial condition,

$$P(y, t=0) = P_i \tag{3.2}$$

outer boundary condition for an infinite-acting system,

$$\lim_{y\to\infty} P(y,t) = P_i \tag{3.3}$$

and the inner boundary condition,

$$q_{sc}\rho_{g,sc} = (6.328\times10^{-3})2x_f h\rho_g \frac{k}{\mu}\left(\frac{\partial P}{\partial y}\right)_{y=0} \tag{3.4}$$

Using the real-gas equation of state,

$$\rho_g = \frac{PM}{zRT} \tag{3.5}$$

and the definition of isothermal gas compressibility,

$$c_g = \left(\frac{1}{P} - \frac{1}{z}\frac{\partial z}{\partial P}\right)_T \tag{3.6}$$

24

Write Equation (3.1) through (3.4) as follows;

$$\frac{\partial}{\partial y}\left(\frac{P}{z}\frac{k}{\mu_g}\frac{\partial P}{\partial y}\right)=\frac{\phi c_g}{6.328\times10^{-3}}\frac{P}{z}\frac{\partial P}{\partial t} \tag{3.7}$$

where the rock compressibility is neglected with respect to compressibility of gas (constant rock porosity).

If the definition of pseudopressure [1] is used;

$$m(P)=\int_{P_b}^{P}\frac{2P'}{\mu z}dP' \tag{3.8}$$

Equation (3.7) can be written as follows;

$$\frac{\partial^2\Delta m}{\partial y^2}=\frac{1}{\eta}\frac{\partial\Delta m}{\partial t} \tag{3.9}$$

where define;

$$\Delta m(P)=m(P_i)-m(P) \tag{3.10}$$

and

$$\eta=\frac{6.328\times10^{-3}k}{\phi\mu_g c_g} \tag{3.11}$$

Similarly, Eqn. (3.2) through (3.4) can be written, respectively, as follows;

25

$$\Delta m(P(y, t = 0)) = 0 \tag{3.12}$$

$$\lim_{y \to \infty} \Delta m(P(y, t)) = 0 \tag{3.13}$$

and

$$\left(\frac{\partial \Delta m}{\partial y} \right)_{y=0} = -\frac{1422\pi q(t)T}{x_f h k} \tag{3.14}$$

For notational simplicity, in Eqn. (3.14), the subscript can be dropped and used $q(t) \equiv q_{sc}(t)$ (that is, in the following derivations, $q(t)$ corresponds to the flow rate in standard conditions). Note that the diffusion equation given by Eqn. (3.9) is nonlinear because η (defined in Eqn. (3.11)) is a function of pseudopressure. Next, the initial boundary value problem (IBVP) given by Eqns. (3.9) and (3.12) through (3.14) is stated as a perturbation problem.

3.2. Formulation of the Perturbation Problem

Define the constant,

$$\eta_i = \frac{6.328 \times 10^{-3} k}{\left(\phi \mu_g c_g \right)_i} \tag{3.15}$$

where the subscript i refers the value of the property at initial pressure. Also, the new parameter is defined,

$$\omega = \omega(y, t) = \frac{\eta_i - \eta}{\eta} = \frac{\left(\mu_g c_g \right)_i - \mu_g c_g}{\mu_g c_g} \tag{3.16}$$

and write Eqn. (3.9) as follows;

26

$$\frac{\partial^2 \Delta m}{\partial y^2} = (1+\omega)\frac{1}{\eta_i}\frac{\partial \Delta m}{\partial t} \tag{3.17}$$

Introducing the small perturbation, ε, Eqn. (3.17) can be expressed in the following form;

$$\frac{\partial^2 \Delta m}{\partial y^2} = (1+\varepsilon\omega)\frac{1}{\eta_i}\frac{\partial \Delta m}{\partial t} \tag{3.18}$$

where

$$\varepsilon = \begin{cases} 0 & \text{Linear problem} \\ 1 & \text{Non-linear problem} \end{cases} \tag{3.19}$$

Together with the initial and boundary conditions (Eqns (3.12) through (3.14)), Eqn. (3.18) defines a perturbation IBVP, which has the perturbation solution in the following form;

$$\Delta m = \Delta m^{(0)} + \sum_{k=1}^{\infty} \varepsilon^{(k)} \Delta m^{(k)} \tag{3.20}$$

Substituting Eqn. (3.20) into Eqn. (3.18), obtain;

$$\left(\frac{\partial^2 \Delta m^{(0)}}{\partial y^2} - \frac{1}{\eta_i}\frac{\partial \Delta m^{(0)}}{\partial t}\right) + \varepsilon^{(1)}\left(\frac{\partial^2 \Delta m^{(1)}}{\partial y^2} - \frac{1}{\eta_i}\frac{\partial \Delta m^{(1)}}{\partial t} - \frac{\omega^{(0)}}{\eta_i}\frac{\partial \Delta m^{(0)}}{\partial t}\right)$$
$$+\varepsilon^{(2)}\left(\frac{\partial^2 \Delta m^{(2)}}{\partial y^2} - \frac{1}{\eta_i}\frac{\partial \Delta m^{(2)}}{\partial t} - \frac{\omega^{(1)}}{\eta_i}\frac{\partial \Delta m^{(1)}}{\partial t}\right) + ... \tag{3.21}$$
$$+\varepsilon^{(k)}\left(\frac{\partial^2 \Delta m^{(k)}}{\partial y^2} - \frac{1}{\eta_i}\frac{\partial \Delta m^{(k)}}{\partial t} - \frac{\omega^{(k-1)}}{\eta_i}\frac{\partial \Delta m^{(k-1)}}{\partial t}\right) + ... = 0$$

Eqn. (3.21) suggests that $\Delta m^{(0)}$, $\Delta m^{(1)}$, $\Delta m^{(2)}$,..., $\Delta m^{(k)}$,... are the solutions of the following set of IBVPs:

0th order perturbation problem:

$$\left.\begin{aligned}
&\frac{\partial^2 \Delta m^{(0)}}{\partial y^2} - \frac{1}{\eta_i}\frac{\partial \Delta m^{(0)}}{\partial t} = 0 \\
&\Delta m^{(0)}(y, t \to 0) = 0 \\
&\Delta m^{(0)}(y \to \infty, t) = 0 \\
&\left(\frac{\partial \Delta m^{(0)}}{\partial y}\right)_{y=0} = -\frac{1422\pi q(t)T}{khx_f}
\end{aligned}\right\} \qquad (3.22)$$

1st order perturbation problem:

$$\left.\begin{aligned}
&\frac{\partial^2 \Delta m^{(1)}}{\partial y^2} - \frac{1}{\eta_i}\frac{\partial \Delta m^{(1)}}{\partial t} - \frac{\omega^{(0)}}{\eta_i}\frac{\partial \Delta m^{(0)}}{\partial t} = 0 \\
&\Delta m^{(1)}(y, t \to 0) = 0 \\
&\Delta m^{(1)}(y \to \infty, t) = 0 \\
&\left(\frac{\partial \Delta m^{(1)}}{\partial y}\right)_{y=0} = 0
\end{aligned}\right\} \qquad (3.23)$$

2nd order perturbation problem:

$$\left.\begin{aligned}
&\frac{\partial^2 \Delta m^{(2)}}{\partial y^2} - \frac{1}{\eta_i}\frac{\partial \Delta m^{(2)}}{\partial t} - \frac{\omega^{(1)}}{\eta_i}\frac{\partial \Delta m^{(1)}}{\partial t} = 0 \\
&\Delta m^{(2)}(y, t \to 0) = 0 \\
&\Delta m^{(2)}(y \to \infty, t) = 0 \\
&\left(\frac{\partial \Delta m^{(2)}}{\partial y}\right)_{y=0} = 0
\end{aligned}\right\} \qquad (3.24)$$

.

.

.

kth order perturbation problem:

$$
\left.
\begin{aligned}
&\frac{\partial^2 \Delta m^{(k)}}{\partial y^2} - \frac{1}{\eta_i}\frac{\partial \Delta m^{(k)}}{\partial t} - \frac{\omega^{(k-1)}}{\eta_i}\frac{\partial \Delta m^{(k-1)}}{\partial t} = 0 \\
&\Delta m^{(k-1)}(y, t \to 0) = 0 \\
&\Delta m^{(k-1)}(y \to \infty, t) = 0 \\
&\left(\frac{\partial \Delta m^{(k-1)}}{\partial y}\right)_{y=0} = 0
\end{aligned}
\right\}
\tag{3.25}
$$

.

.

.

3.3. Solution of the Perturbation Problem

The solution of the perturbation problem defined in Section 3.2 is obtained by finding the individual solutions for each of the kth order ($k = 0, 1, \ldots$) perturbation problem and substituting into Eqn. (3.20). Below, the solution of the 0th and the 1st order perturbation problems are demonstrated. The same procedure used to solve the 1st order perturbation problem can be applied to the higher order perturbation problems. However, the solutions for the higher order perturbation problems becomes more complex and computationally more cumbersome. Moreover, as noted by Barreto et al. [2] [3] and Ahmadi [5], including the first order perturbation yields sufficiently accurate results for most practical purposes. Therefore, in this work, the perturbation solution will be truncated after the first order perturbation.

3.3.1. Solution of the 0th Order Perturbation Problem (Linear Problem)

Consider the 0th order perturbation problem (the linear problem) given by Eqn. (3.22) and repeated below for convenience:

$$\frac{\partial^2 \Delta m^{(0)}}{\partial y^2} - \frac{1}{\eta_i}\frac{\partial \Delta m^{(0)}}{\partial t} = 0 \qquad (3.26)$$

$$\Delta m^{(0)}(y, t \to 0) = 0 \qquad (3.27)$$

$$\Delta m^{(0)}(y \to \infty, t) = 0 \qquad (3.28)$$

and

$$\left(\frac{\partial \Delta m^{(0)}}{\partial y}\right)_{y=0} = -\frac{1422\pi q(t)T}{khx_f} \qquad (3.29)$$

The Green's function solution of the linear problem (Eqns. (3.26)-(3.29)) is given by;

$$\Delta m^{(0)}(y,t) = -\eta_i \int_0^t \int_0^\infty \left[G(y-y',t-\tau)\left(\frac{\partial^2 \Delta m^{(0)}}{\partial y'^2}\right)_{(y',\tau)} - \Delta m^{(0)}(y',\tau)\left(\frac{\partial^2 G}{\partial y'^2}\right)_{(y-y',t-\tau)} \right] dy' d\tau \qquad (3.30)$$

where the Green's function is given by [49] [50],

$$G(y-y',t-\tau) = \frac{1}{2\sqrt{\pi\eta_i(t-\tau)}}\exp\left(-\frac{(y-y')^2}{4\eta_i(t-\tau)}\right) \qquad (3.31)$$

Using Green's second identity (divergence theorem), Eqn. (3.30) can be written as follows;

$$\Delta m^{(0)}(y,t) = -\eta_i \int_0^t \left(G\frac{\partial \Delta m^{(0)}}{\partial y'} - \Delta m^{(0)}\frac{\partial G}{\partial y'} \right)\Bigg|_0^\infty d\tau \qquad (3.32)$$

By Eqn. (3.28), both G and $\Delta m^{(0)}$ disappear $y, y' \rightarrow \infty$ and $\left(\partial \Delta m^{(0)}/\partial y\right)_{y=0}$ is given by Eqn. (3.29). Thus, from Eqn. (3.32), the solution of the 0th order perturbation problem is obtained as follows;

$$\Delta m^{(0)}\left(y,t\right) = \frac{1422T\sqrt{\pi\eta_i}}{2khx_f} \int_0^t \frac{q(\tau)}{\sqrt{t-\tau}} \exp\left(-\frac{y^2}{4\eta_i(t-\tau)}\right) d\tau \tag{3.33}$$

Note that, if $q(t) = q = \text{Constant}$, then Eqn. (3.33) yields the following well-known, 1D, infinite-conductivity fracture solution [50];

$$
\begin{aligned}
\Delta m^{(0)}\left(y,t\right) &= \frac{1422qT\sqrt{\pi\eta_i}}{2khx_f} \int_0^t \frac{1}{\sqrt{t-\tau}} \exp\left(-\frac{y^2}{4\eta_i(t-\tau)}\right) d\tau \\
&= \frac{1422qT}{kh} \left[\sqrt{\frac{\pi\eta_i t}{x_f^2}} \exp\left(-\frac{y^2}{4\eta_i t}\right) - \frac{\pi y}{2x_f} erfc\left(\frac{y}{2\sqrt{\eta_i t}}\right) \right]
\end{aligned} \tag{3.34}
$$

3.3.2. Solution of the 1st Order Perturbation Problem

Now, consider the 1st order perturbation problem (Eqn. (3.23)) rewritten below for convenience;

$$\frac{\partial^2 \Delta m^{(1)}}{\partial y^2} - \frac{1}{\eta_i} \frac{\partial \Delta m^{(1)}}{\partial t} - \frac{\omega^{(0)}}{\eta_i} \frac{\partial \Delta m^{(0)}}{\partial t} = 0 \tag{3.35}$$

$$\Delta m^{(1)}(y, t \rightarrow 0) = 0 \tag{3.36}$$

$$\Delta m^{(1)}(y \rightarrow \infty, t) = 0 \tag{3.37}$$

and

$$\left(\frac{\partial \Delta m^{(1)}}{\partial y} \right)_{y=0} = 0 \qquad (3.38)$$

The Green's function solution of the problem in Eqns. (3.35) through (3.38) is given by,

$$\Delta m^{(1)}(y,t) = -\eta_i \int_0^t \int_0^\infty \left[G \left(\frac{\partial^2 \Delta m^{(1)}}{\partial y'^2} - \frac{\omega^{(0)}}{\eta_i} \frac{\partial \Delta m^{(0)}}{\partial \tau} \right) - \Delta m^{(1)} \frac{\partial^2 G}{\partial y'^2} \right] dy' d\tau \qquad (3.39)$$

which can be rearranged as follows;

$$\Delta m^{(1)}(y,t) = -\eta_i \int_0^t \int_0^\infty \left[\left(G \frac{\partial^2 \Delta m^{(1)}}{\partial y'^2} - \Delta m^{(1)} \frac{\partial^2 G}{\partial y'^2} \right) - G \frac{\omega^{(0)}}{\eta_i} \frac{\partial \Delta m^{(0)}}{\partial \tau} \right] dy' d\tau \qquad (3.40)$$

Using the Green's second identity yields;

$$\Delta m^{(1)}(y,t) = -\eta_i \int_0^t \left(G \frac{\partial \Delta m^{(1)}}{\partial y'} - \Delta m^{(1)} \frac{\partial G}{\partial y'} \right) \Bigg|_0^\infty d\tau + \int_0^t \int_0^\infty G \omega^{(0)} \frac{\partial \Delta m^{(0)}}{\partial \tau} dy' d\tau \qquad (3.41)$$

From Eqn. (3.33);

$$\left(\frac{\partial \Delta m^{(0)}}{\partial t} \right)_{(y',t')} = \frac{1422 T \sqrt{\pi \eta_i}}{2khx_f} \frac{q(\tau)}{\sqrt{t-\tau}} \exp\left(-\frac{y'^2}{4\eta_i(t-\tau)} \right) \qquad (3.42)$$

Substituting Eqns. (3.31) and (3.42) into Eqn. (3.41), the following solution for the 1st order perturbation problem is obtained:

$$\Delta m^{(1)}(y,t) = \frac{1422 T}{4khx_f} \int_0^t \frac{q(\tau)}{t-\tau} \int_0^\infty \omega^{(0)}(y',\tau) \exp\left(-\frac{(y-y')^2 + y'^2}{4\eta_i(t-\tau)} \right) dy' d\tau \qquad (3.43)$$

32

3.3.3. Truncated Perturbation Solution

As noted in the beginning of this section, based on the observations of Barreto et al. [2] [3] and Ahmadi [5], the solution derived here will be truncated after the first perturbation term. Therefore, using Eqns. (3.33) and (3.43) in Eqn. (3.20), the following truncated perturbation solution for the fractured tight-gas well problem is obtained:

$$\Delta m(y,t) = \frac{1422T}{2khx_f} \left\{ \begin{array}{l} \displaystyle\int_0^t \frac{q(\tau)\sqrt{\pi\eta_i}}{\sqrt{t-\tau}} \exp\left(-\frac{y^2}{4\eta_i(t-\tau)}\right) d\tau \\[4mm] \displaystyle+\int_0^t \frac{q(\tau)}{2(t-\tau)} \int_0^\infty \omega^{(0)}(y',\tau) \exp\left(-\frac{(y-y')^2 + y'^2}{4\eta_i(t-\tau)}\right) dy' d\tau \end{array} \right\} \tag{3.44}$$

Computation of the perturbation solution obtained here requires numerical evaluation of the integrals involved in Eqn. (3.44). Computation of the semi-infinite space integral particularly poses difficulties. Procedures described by Barreto et al. [2] [3] and Ahmadi [5] are useful in the numerical evaluation of the integrals in Eqn. (3.44). In the next section, the procedure used to compute Eqn. (3.44) will be described and the numerical results will be compared with the existing semi-analytical and numerical results to verify the solution.

3.4. Computation and Verification of the Truncated Solution

The numeric computation of truncated perturbation solution (Eqn. (3.44)) represents semi-infinite space integration and multidimensional numerical integration which acquires some difficulties. In order to perform numeric integration Matlab [51] was used.

If the truncated perturbation solution is evaluated at the surface of the fracture ($y=0$), Eqn. (3.44) becomes;

$$\Delta m(0,t) = \frac{1422T}{2khx_f} \left\{ \begin{array}{l} \int_0^t \frac{q(\tau)\sqrt{\pi\eta_i}}{\sqrt{t-\tau}} d\tau \\[4mm] + \int_0^t \frac{q(\tau)}{2(t-\tau)} \int_0^\infty \omega^{(0)}(y',\tau) \exp\left(-\frac{y'^2}{2\eta_i(t-\tau)}\right) dy' d\tau \end{array} \right\} \tag{3.45}$$

The first term in Eqn. (3.45) is the 0th order perturbation solution ($\Delta m^{(0)}$) which is the exact solution to the linear problem. 0th order perturbation solution is the conventional solution of the gas diffusivity equation in which we assume that the pseudopressure approach can linearize the gas diffusion equation. One of the significant assumptions in the use of pseudopressure transformation is that small variations in pressure cause small variations in viscosity-compressibility product and this nonlinearity can be handled by pseudopressure transformation. The 0th order perturbation solution at the fracture surface can be given by;

$$\Delta m^{(0)}(0,t) = \frac{1422T}{2khx_f} \int_0^t \frac{q(\tau)\sqrt{\pi\eta_i}}{\sqrt{t-\tau}} d\tau \tag{3.46}$$

The second term in Equation (3.45) is the 1st order perturbation solution ($\Delta m^{(1)}$) and is added to the exact solution of the linear problem to take into account the effect in the change of viscosity and compressibility under large pressure variations. The 1st order perturbation solution at the fracture surface can be written;

$$\Delta m^{(1)}(0,t) = \frac{1422T}{4khx_f} \left\{ \int_0^t \frac{q(\tau)}{(t-\tau)} \int_0^\infty \omega^{(0)}(y',\tau) \exp\left(-\frac{y'^2}{2\eta_i(t-\tau)}\right) dy' d\tau \right\} \tag{3.47}$$

For the verification of the numerical solution of the truncated perturbation solution, Thompson's spectral solution [40] and Eclipse [39] were used.

For the calculation of gas properties like viscosity and gas compressibility different correlations were used and are shown in Table 3.1. Sutton's associated gas correlations

[52] were used for pseudo critical pressure and temperature. For gas deviation factor and compressibility, Azizi et al. [53] correlations were utilized. Gas viscosity was estimated from Lee et al. correlations [54]. Same gas property correlations were used for spectral solution [40], truncated perturbation solution and for Eclipse [39].

Table 3.1. The correlations used for the evaluation of gas properties

T_{pc}, P_{pc}	Sutton's associated gas correlations [52]
z-factor, c_g	Azizi et al. correlations [53]
μ_g	Lee et al. correlations [54]

Two synthetic data sets (Case 1 and Case 2) were created in spectral solution [40] and Eclipse [39]. For both of the cases, fracture conductivity is infinite and the flow to the fracture is linear, that is, the reservoir is in infinite-acting period for all the production period. Similar reservoir rock and fluid properties was implemented for both of the cases as given in Table 3.2. However, production pressures and flow rates differ for two cases. For the first case (Case 1), constant bottomhole production pressure and variable production rates were selected, while for the second case (Case 2), variable pressure and variable rate production was enforced as an inner boundary conditions.

Table 3.2. Reservoir rock and fluid data for Case 1 and Case 2

Matrix permeability, k, mD	0.0001
Matrix porosity, ϕ	0.064
Fracture height, h, ft	100
Fracture half length, x_f, ft	100
Reservoir length, L_e, ft	1000
Initial reservoir pressure, P_i, psia	10000
Reservoir temperature, T, °F	200
Gas specific gravity, SG	0.71

3.4.1. Case 1 - Constant bottomhole pressure case

For the first case, the wellbore pressure and the corresponding production rate obtained from Eclipse were shown in Figure 3.2.
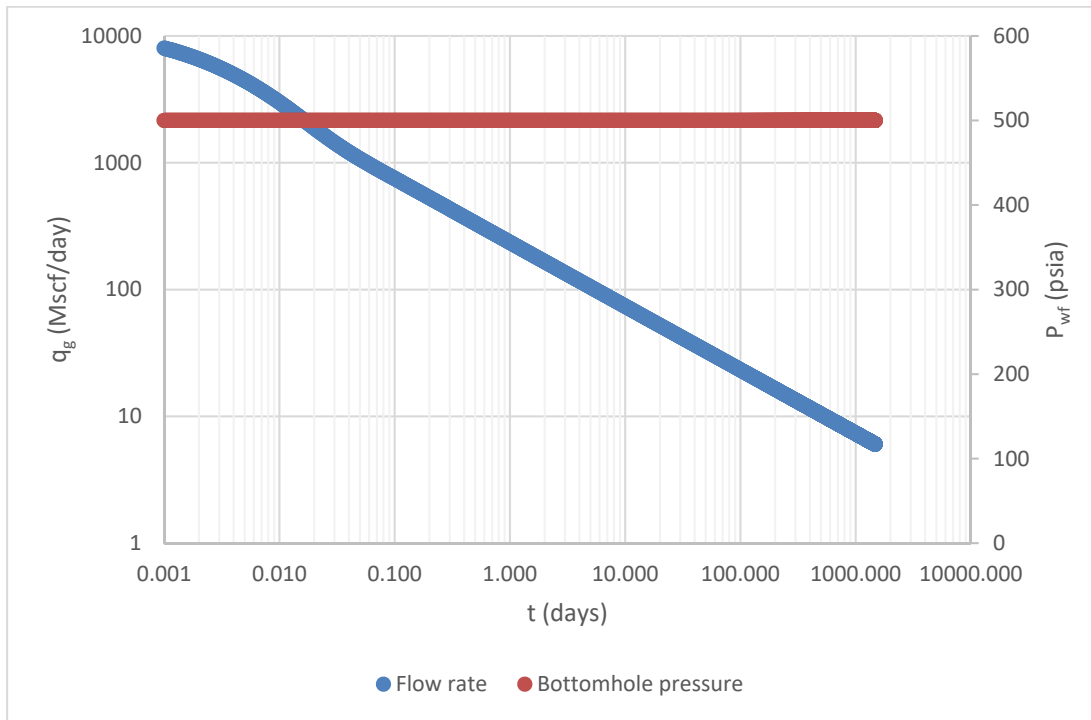
Figure 3.2. Wellbore pressures and flow rates obtained from Eclipse with respect to time for Case 1

The wellbore pressures and the corresponding flow rates obtained from spectral solution [40] can be seen from Figure 3.3.

36
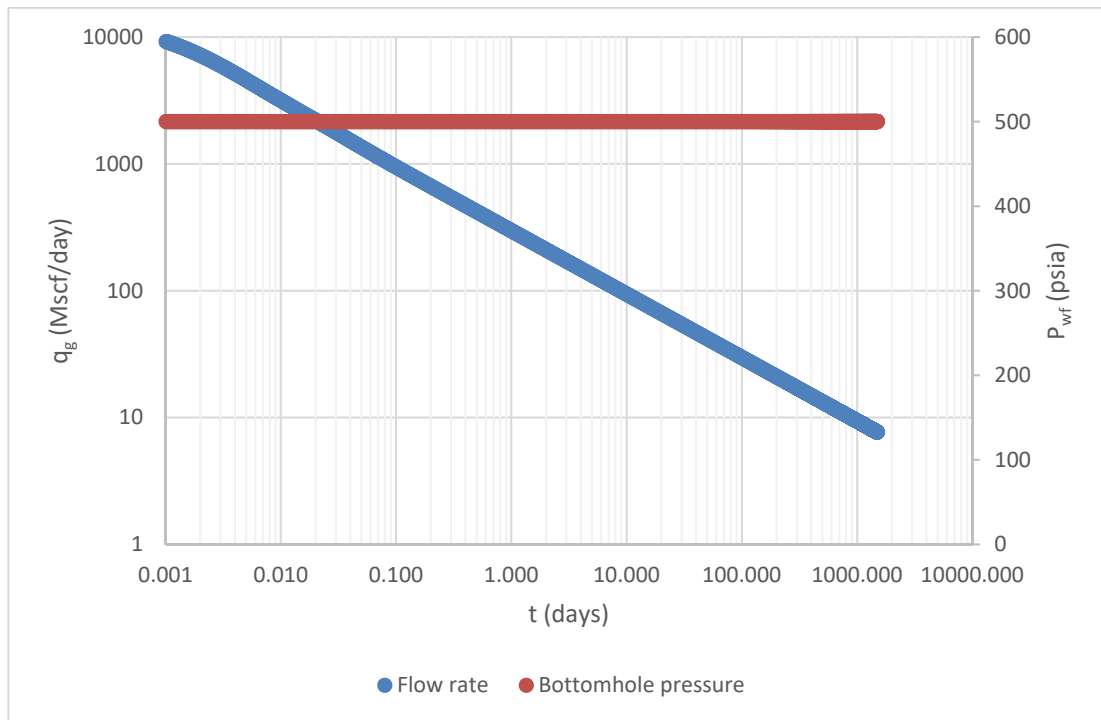
Figure 3.3. Wellbore pressures and flow rates obtained from spectral solution with respect to time for Case 1

The comparison of the flow rates obtained from Eclipse and spectral solution [40] can be seen from Figure 3.4. The numerical simulator gives lower values in flow rate compared to spectral solution. The reason behind this can be the grid refinement, because of the grid size limitations, the finite difference simulators cannot capture the variation in viscosity and compressibility in the near vicinity of the fracture. However, it must be emphasized that the conclusions drawn here are not about the particular choice of a simulator, they are about comparing the finite difference methods and the spectral methods. Because of the grid requirements, finite difference simulators require excessive grid refinement in order to catch the near analytical accuracy of spectral method. The grid sizes near the surface of the fracture implemented in Eclipse can be seen in Figure 3.5.
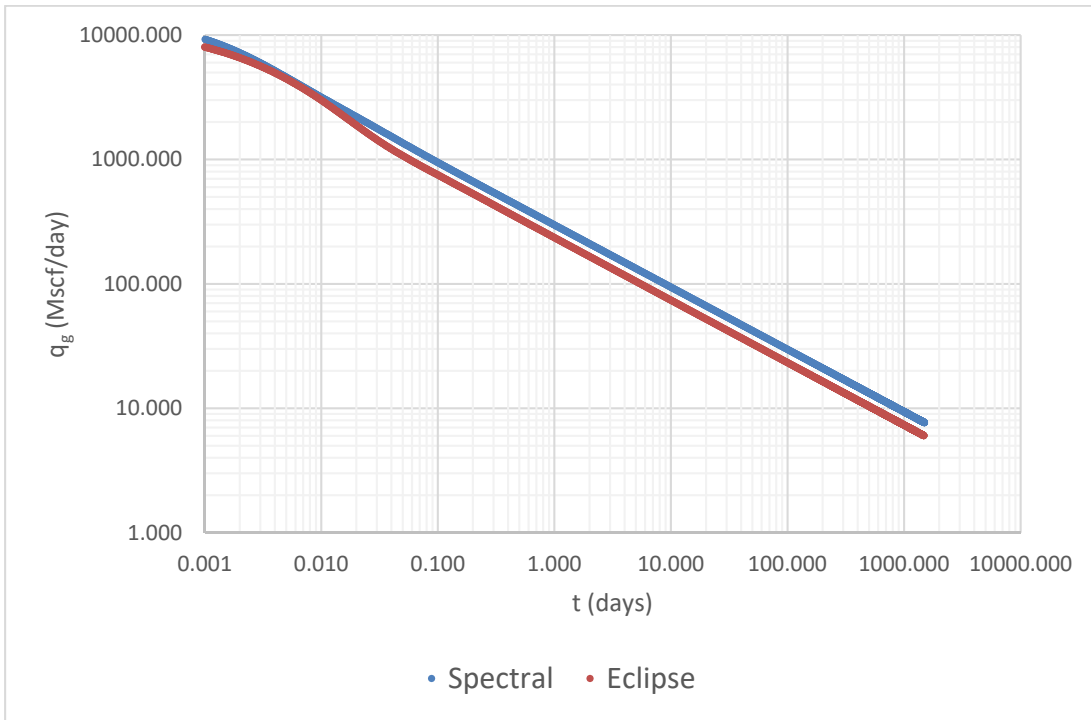
Figure 3.4. Comparison of Eclipse and spectral solution flow rates for Case 1
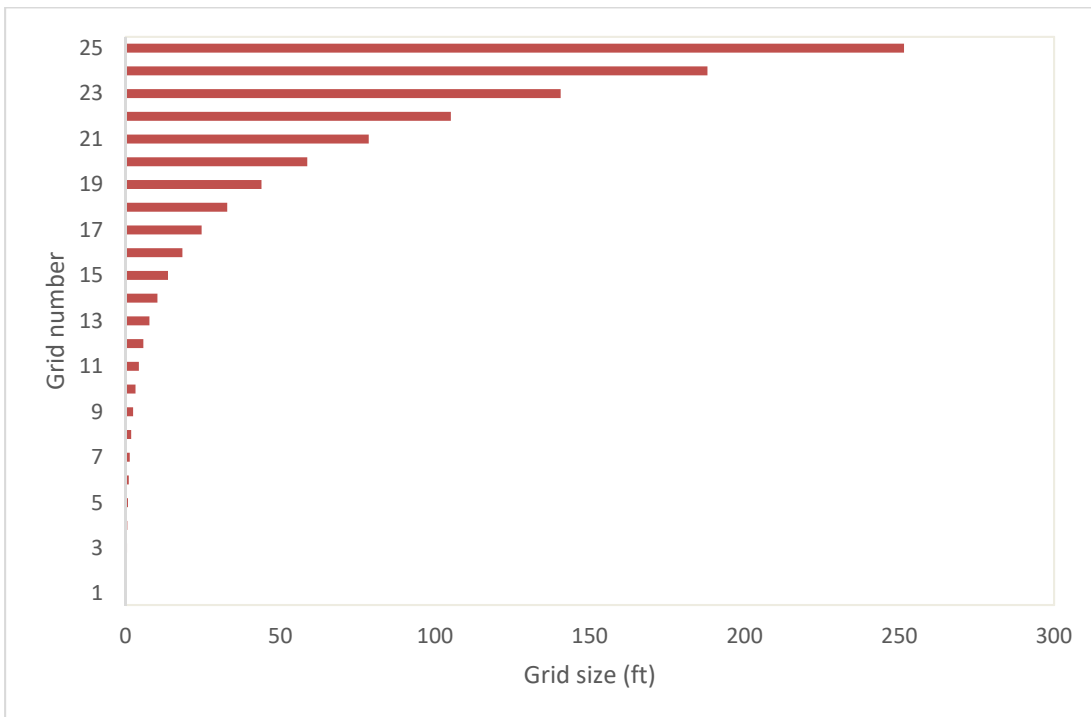
Figure 3.5. Logarithmic gridding in Eclipse

In Figure 3.6, the pseudopressure drops obtained from numerical solution of truncated perturbation solution (Eqn. (3.45)) are compared with the Thompson's spectral solution [40] and Eclipse. In order to calculate pseudopressure drops from Eclipse, Al-Hussainy et al. [1] pseudopressure equation is used and the gas properties were calculated according to the above mentioned correlations [52] [53] [54]. After initial flow period, the pseudopressure drops obtained from numerical solution of truncated perturbation solution, spectral solution and Eclipse are matched admirably.
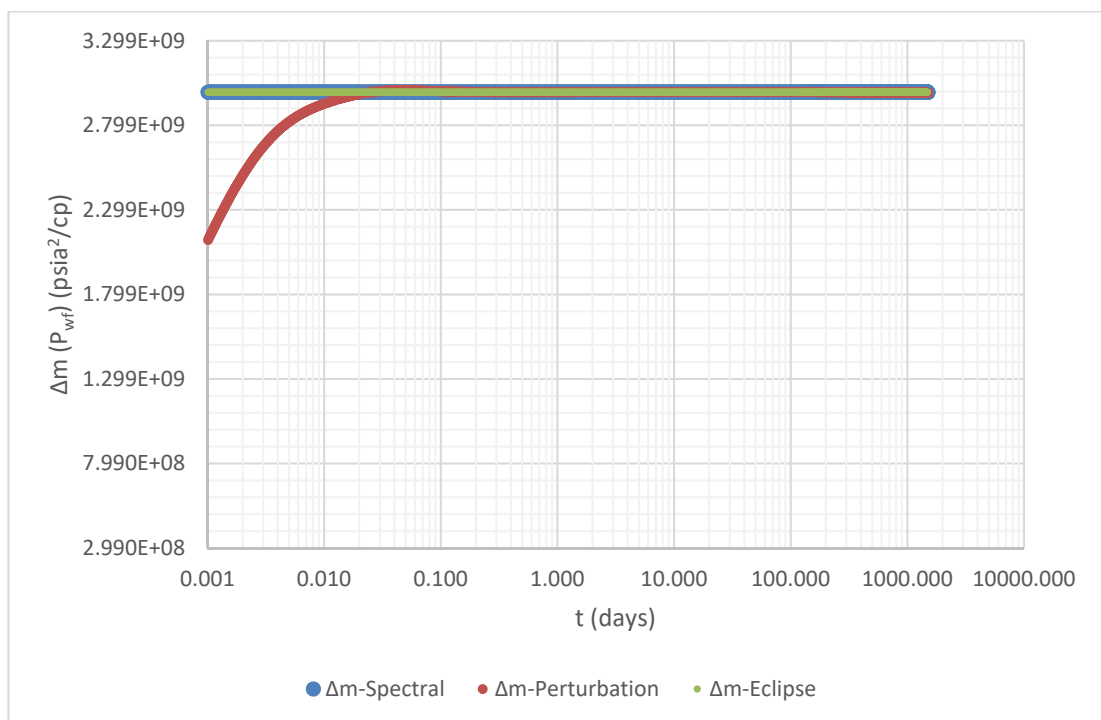
Figure 3.6. Comparison of pseudopressure drops for numerical solution of truncated perturbation solution, spectral solution and Eclipse for Case 1

The perturbation technique allows us to see the deviation from the exact solution. It separates the problem into a series of linear problems. The 0th order perturbation is the exact solution of the gas diffusivity equation which assumes the diffusion equation is linear. The 0th order perturbation solution is the conventional solution of the gas diffusivity equation. The 1st order perturbation term is added to the exact solution. Therefore, the truncated perturbation solution takes into account the large variation in viscosity-compressibility product. In other words, from 1st order perturbation, we can

see the deviation from the exact solution. The 0th, 1st order perturbation and truncated perturbation solutions can be seen in Figure 3.7.
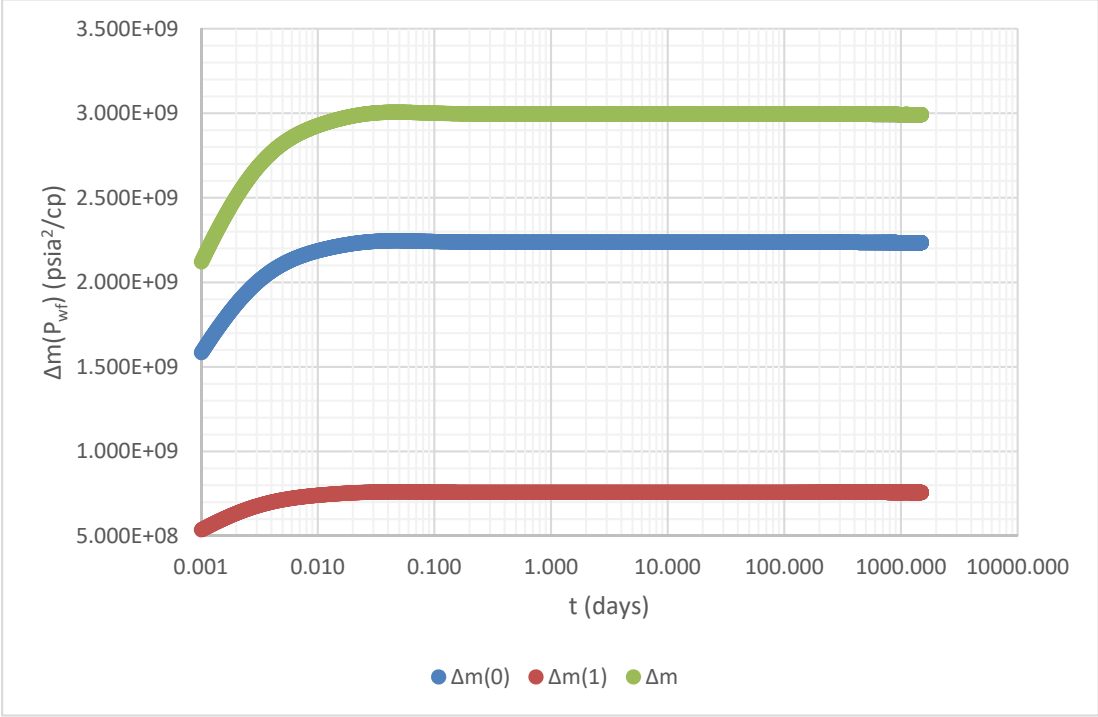
Figure 3.7. The 0th and 1st order perturbation results for the numeric evaluation of truncated perturbation solutions for Case 1

It can be obviously seen from Figure 3.7, the exact solution ($\Delta m^{(0)}$) leads to lower pseudopressure drops. In 0th order perturbation solution the assumption is that the small variations in pressure cause small variations in viscosity-compressibility product and these variations can be managed by pseudopressure. However, in this case there occurs a huge pressure drop at the surface of the fracture and evaluating this pressure drop with pseudopressure technique does not create convincingly accurate results since the nonlinearity cannot be handled by the pseudopressure transformation technique. The 1st order perturbation solution result shows the correction term that is added to 0th order perturbation solution. The total solution, i.e. the truncated perturbation solution, takes into account the large variation in viscosity and compressibility with pressure. Therefore, by looking at Figure 3.7, it can be deduced

that in fractured tight gas wells when large pressure drops occur using conventional linear flow equations leads us to lower estimates in pseudopressure drops.

In Figure 3.8, change in gas diffusivity deviation factor ($\omega^{(0)}$) can be seen. According to Eqn. (3.16), gas diffusivity deviation factor indicates the deviation of viscosity-compressibility product from its initial state and it changes between $-1 < \omega^{(0)} < 0$. $\omega^{(0)} = 0$ means that there is no change in viscosity-compressibility product; that is there is no deviation from the slightly compressible fluid case. However, as it is getting smaller, the deviation from slightly compressible fluid case is increasing. In Case 1, constant bottomhole pressure production case, there is a huge pressure drop from initial reservoir pressure ($P_i = 10\ 000$ psia) to well bottomhole pressure ($P_{wf} = 500$ psia). Under this large pressure change, there occurs a huge variation in viscosity-compressibility product. As can be seen from Figure 3.8, $\omega^{(0)}$ changes abruptly to almost its smallest value and becomes constant since the wellbore pressure is constant.
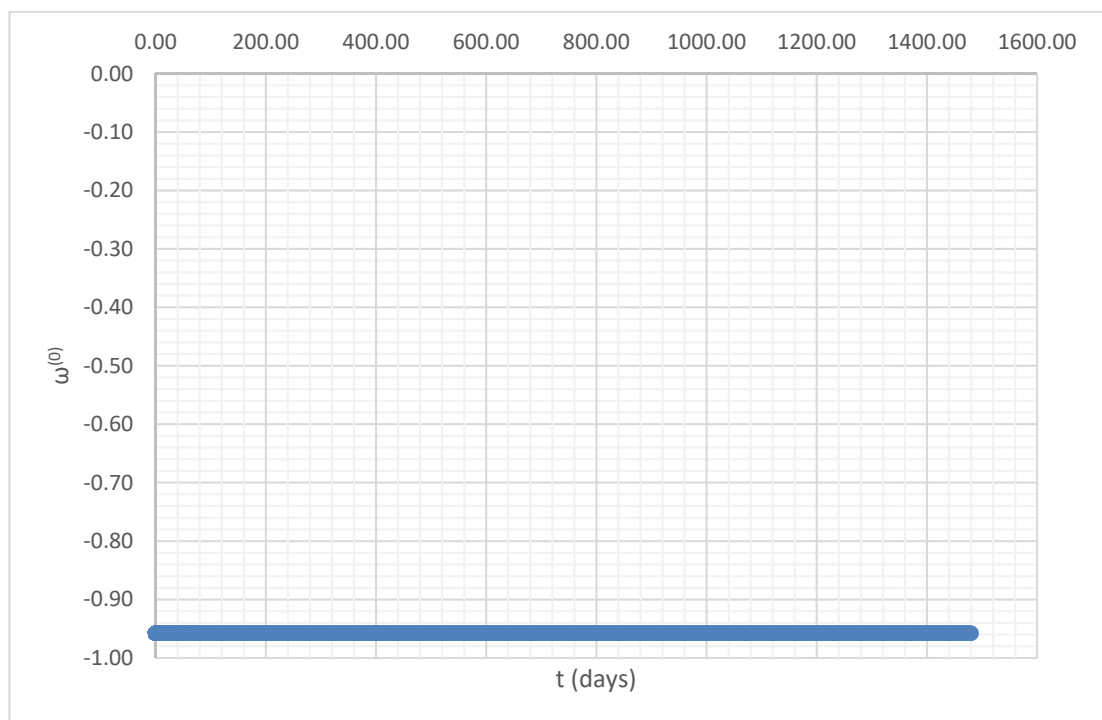
Figure 3.8. Diffusivity gas deviation factor, $\omega^{(0)}$ with respect to time for Case 1

41

3.4.2. Case 2 - Variable bottomhole pressure case

The wellbore pressures and the flow rates obtained from Eclipse for Case 2 can be seen in Figure 3.9
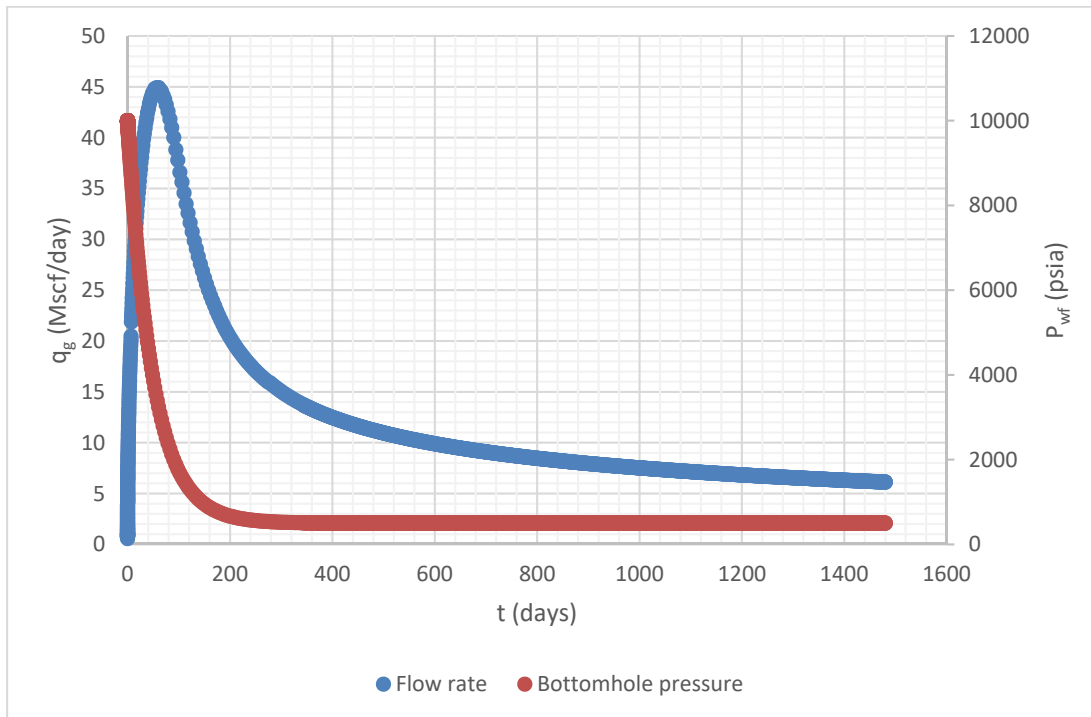
Figure 3.9. Wellbore pressure and flow rate obtained from Eclipse with respect to time for Case 2

The wellbore pressures and the corresponding flow rates obtained from spectral solution [40] can be seen in Figure 3.10.
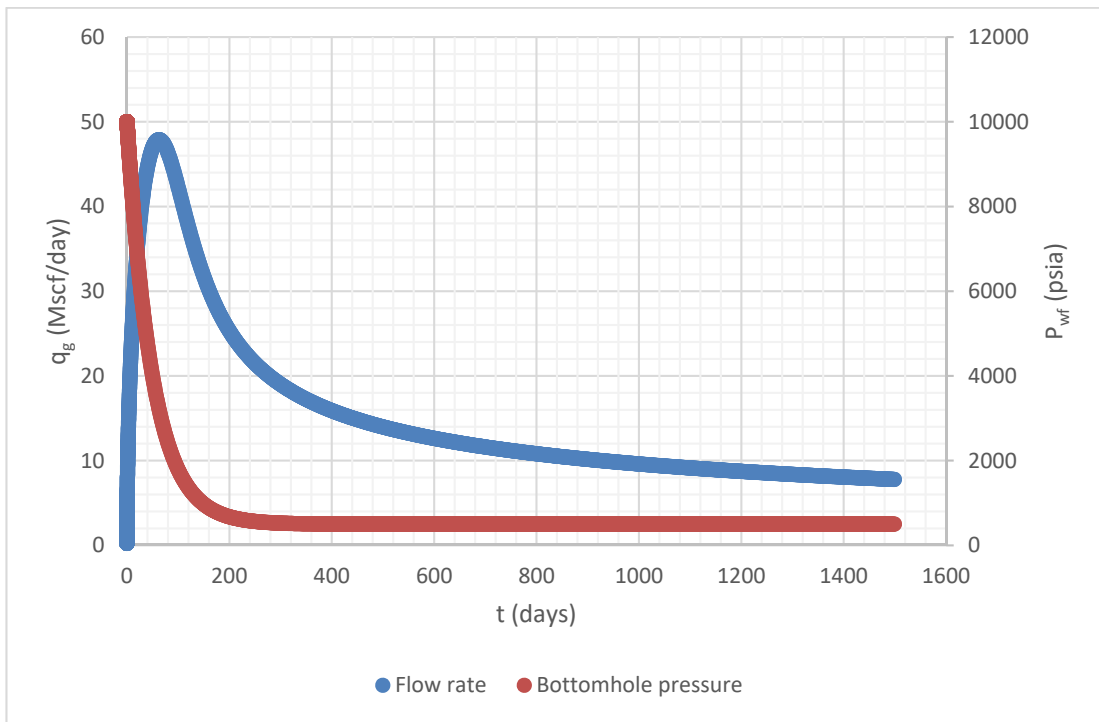
Figure 3.10. Wellbore pressures and the flow rates obtained from spectral solution with respect to time for Case 2

The Eclipse flow rates and the spectral solution flow rates are compared in Figure 3.11. The reason behind the difference in flow rates can be again because of the grid size limitations in finite difference simulators. Same grid sizes were used as in Case 1.
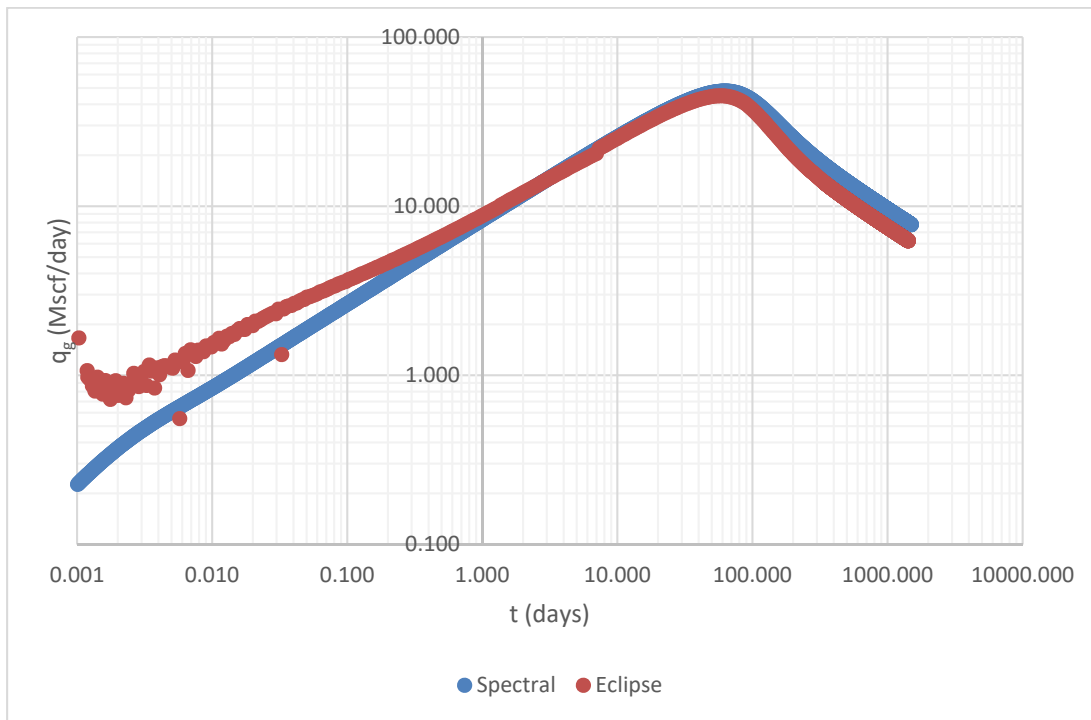
Figure 3.11. Comparison of Eclipse and spectral solution flow rates for Case 2

The pseudopressure drops obtained from numerical solution of truncated perturbation solution (Eqn. (3.45)) are compared with the spectral solution [40] and Eclipse. The results can be seen in Figure 3.12. It can be deduced from Figure 3.12 that after some time, there is a good match between the numerical solution of the truncated perturbation solution, Eclipse and the spectral solution [40].
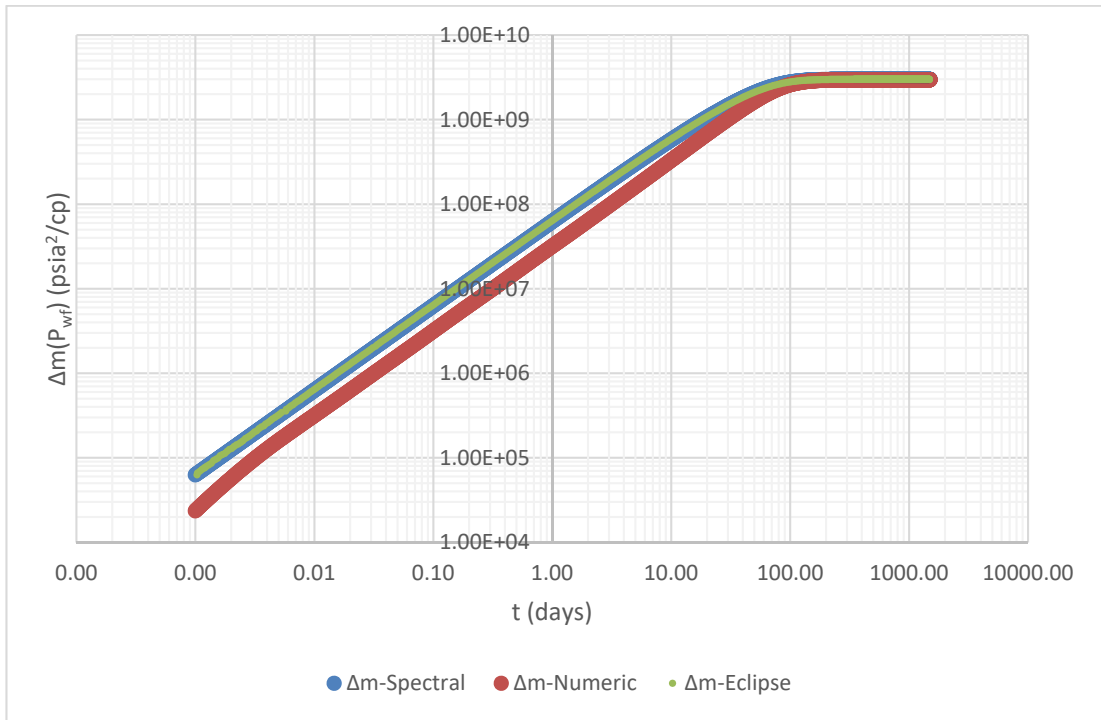
Figure 3.12. Comparison of pseudopressure drops between numerical solution of truncated perturbation solution, spectral solution and Eclipse for Case 2

The pseudopressure drop for 0th order, 1st order and truncated perturbation solutions are seen in Figure 3.13 for Case 2.
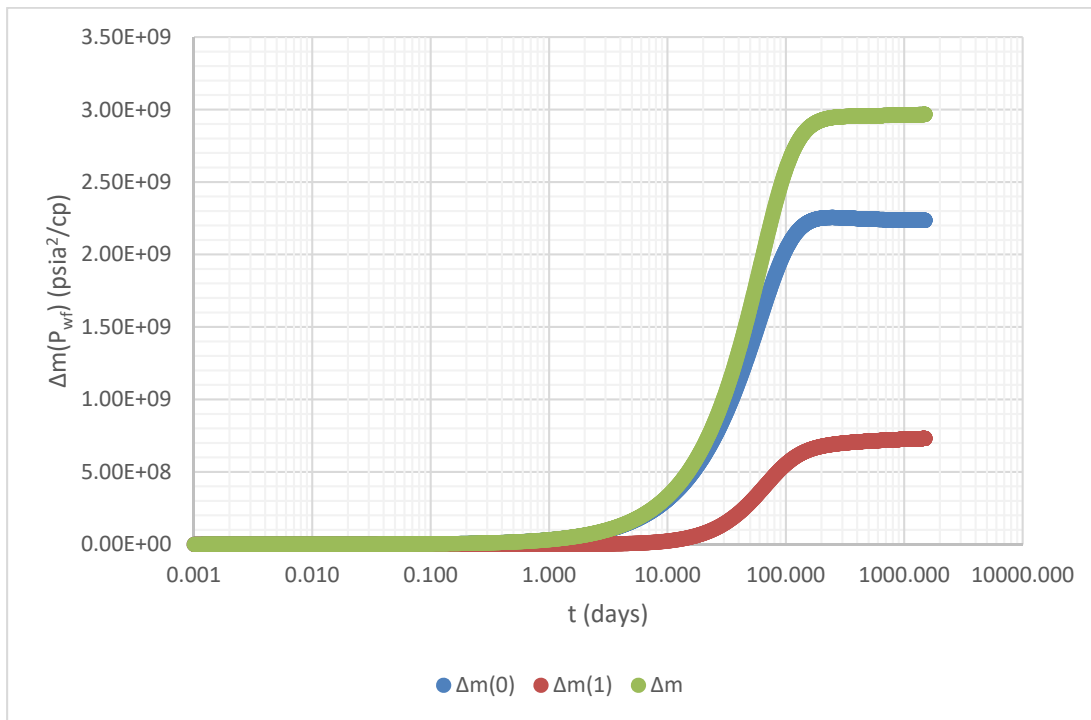
Figure 3.13. The 0th and 1st order perturbation results for the numeric evaluation of truncated perturbation solutions for Case 2

Similar conclusions can be deduced for Case 2. It can be obviously seen from Figure 3.13 that not accounting the effect of large variations in viscosity-compressibility results in misinterpretations. 1st order perturbation solution shows the deviation from the constant viscosity-compressibility product assumption. The nonlinearity of the diffusion equation cannot be neglected in fractured tight-gas wells where high pressure drops are required in order to produce the stored gas in this tiny little pores.

Gas diffusivity deviation factor, seen in Figure 3.14, shows not steep change as in Case 1 but it gradually gets smaller in this case as a result of gradual change in bottomhole pressure.
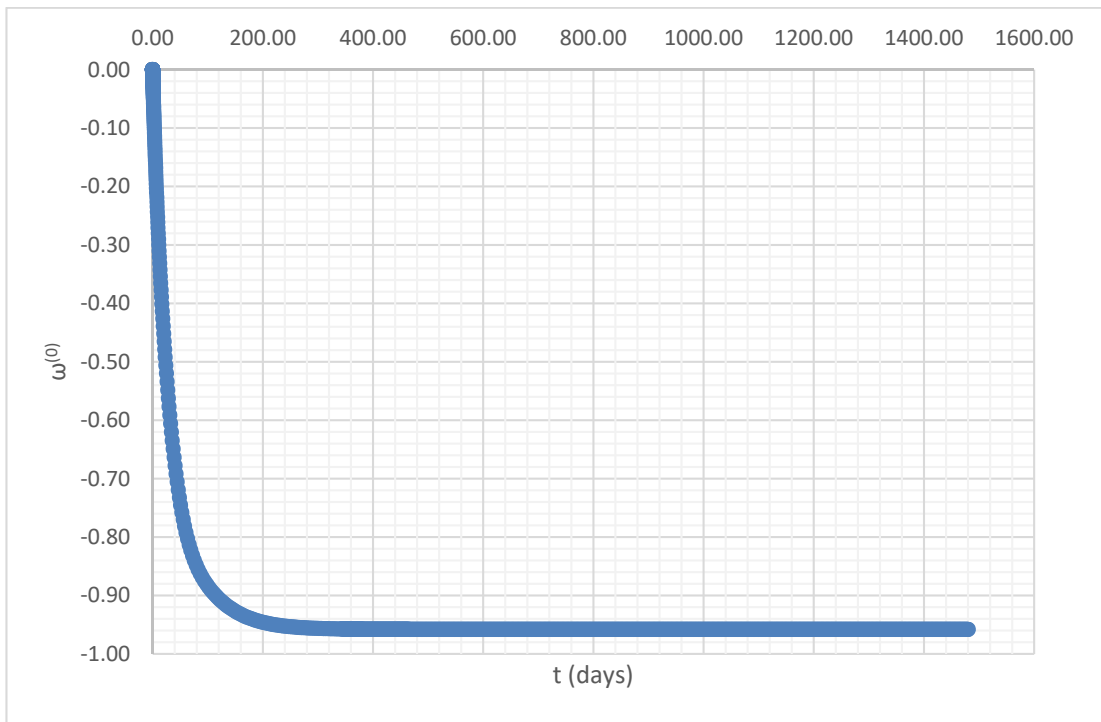
Figure 3.14. Gas diffusivity deviation factor, ω with respect to time for Case 2

CHAPTER 4

APPROXIMATION OF THE GREEN'S FUNCTION SOLUTION

As noted in the Introduction, one of the objectives of deriving an analytical solution for fractured tight-gas wells is to offer a robust tool for quick performance evaluations and provide a sound ground for practical data analysis techniques. The truncated perturbation solution developed in Chapter 3 (Eqn. (3.44)) is not completely satisfactory for these purposes. For example, even to compute the solution at the fracture plane ($y = 0$), pressures would have to be computed at every point in the reservoir because the evaluation of the semi-infinite integral in Eqn. (3.44) requires the ω term (that is, the diffusivity, η) as a function of pressure at every point in the reservoir. Therefore, in this chapter, an approximation of the perturbation-Green's function solution will be derived to improve its practical utility. Our scope here is limited to deriving an approximation for the pressure at the fracture plane ($y = 0$).

4.1. Discretization of Integrals

The first step toward obtaining a more computationally convenient form of the solution is to discretize and find appropriate analytical approximations for the integrals in the solution. First discretize the time integral in Eqn. (3.44) to obtain;

$$\Delta m(y,t) \approx \frac{1422T}{2khx_f} \left\{ \begin{array}{l} \displaystyle\sum_{j=0}^{M-1} q(\tilde{t}_j) \int_{t_j}^{t_{j+1}} \frac{\sqrt{\pi\eta_i}}{\sqrt{t-\tau}} \exp\left(-\frac{y^2}{4\eta_i(t-\tau)}\right) d\tau \\[3mm] + \displaystyle\sum_{j=0}^{M-1} q(\tilde{t}_j) \int_{t_j}^{t_{j+1}} \frac{1}{2(t-\tau)} \int_0^\infty \omega^{(0)}(y',\tau)\exp\left(-\frac{(y-y')^2 + y'^2}{4\eta_i(t-\tau)}\right) dy'\,d\tau \end{array} \right\} \tag{4.1}$$

where $q\left(\tilde{t}_j\right)$ is the mean value of $q(\tau)$ in the interval $t_j < \tau < t_{j+1}$. Similarly, discretizing the space integral in Eqn. (4.1), yields;

$$\Delta m(y,t) \approx \frac{1422T}{2khx_f} \left\{ \begin{array}{l} \displaystyle\sum_{j=0}^{M-1} q(\tilde{t}_j) \int_{t_j}^{t_{j+1}} \frac{\sqrt{\pi\eta_i}}{\sqrt{t-\tau}} \exp\left(-\frac{y^2}{4\eta_i(t-\tau)}\right) d\tau \\ + \displaystyle\sum_{j=0}^{M-1} q(\tilde{t}_j) \lim_{N\to\infty} \sum_{i=0}^{N} \omega^{(0)}\left(\tilde{y_i},\tilde{t}_j\right) \int_{t_j}^{t_{j+1}} \frac{1}{2(t-\tau)} \int_{y_i}^{y_{i+1}} \exp\left(-\frac{(y-y')^2+y'^2}{4\eta_i(t-\tau)}\right) dy' d\tau \end{array} \right\} \quad (4.2)$$

In Eq. 4.2, where $\omega^{(0)}\left(\tilde{y_i},\tilde{\tau}_j\right)$ is the mean value of $\omega^{(0)}(y',\tau)$ in the space interval $y'_j < y' < y'_{j+1}$ and time interval $t_j < \tau < t_{j+1}$. If Eqn. (4.2) is evaluated on the fracture plane ($y = 0$), and have;

$$\Delta m(0,t) \approx \frac{1422T}{2khx_f} \left\{ \begin{array}{l} \displaystyle\sum_{j=0}^{M-1} q(\tilde{t}_j) \int_{t_j}^{t_{j+1}} \frac{\sqrt{\pi\eta_i}}{\sqrt{t-\tau}} d\tau \\ + \displaystyle\sum_{j=0}^{M-1} q(\tilde{t}_j) \lim_{N\to\infty} \sum_{i=0}^{N} \omega^{(0)}\left(\tilde{y_i},\tilde{t}_j\right) \int_{t_j}^{t_{j+1}} \frac{1}{2(t-\tau)} \int_{y_i}^{y_{i+1}} \exp\left(-\frac{y'^2}{2\eta_i(t-\tau)}\right) dy' d\tau \end{array} \right\} \quad (4.3)$$

Consider

$$\int_{y_i}^{y_{i+1}} \exp\left(-\frac{y'^2}{2\eta_i(t-\tau)}\right) dy' \quad (4.4)$$

and make the substitution;

$$u = \frac{y'}{\sqrt{2\eta_i(t-\tau)}}; \quad du = \frac{dy'}{\sqrt{2\eta_i(t-\tau)}}; \quad dy' = \sqrt{2\eta_i(t-\tau)}\,du \quad (4.5)$$

and have;

50

$$\int\limits_{y_i^{'}}^{y_{i+1}^{'}} \exp\left(-\frac{y^{'2}}{2\eta_i(t-\tau)}\right)dy' = \sqrt{\frac{\pi\eta_i(t-\tau)}{2}}\left[erfc\left(\frac{y_i^{'}}{\sqrt{2\eta_i(t-\tau)}}\right)-erfc\left(\frac{y_{i+1}^{'}}{\sqrt{2\eta_i(t-\tau)}}\right)\right] \quad (4.6)$$

Substituting Eqn. (4.6) into Eqn. (4.3) yields;

$$\Delta m(0,t) \approx \frac{1422T}{2khx_f}\left\{\begin{array}{l}\sum\limits_{j=0}^{M-1}q(\tilde{t}_j)\int\limits_{t_j}^{t_{j+1}}\frac{\sqrt{\pi\eta_i}}{\sqrt{t-\tau}}d\tau \\[4mm] +\sum\limits_{j=0}^{M-1}q(\tilde{t}_j)\lim\limits_{N\to\infty}\sum\limits_{i=0}^{N}\omega^{(0)}\left(\tilde{y}_i,\tilde{t}_j\right) \\[4mm] \int\limits_{t_j}^{t_{j+1}}\frac{\sqrt{\pi\eta_i}}{2\sqrt{2}(t-\tau)}\left[erfc\left(\frac{y_i^{'}}{\sqrt{2\eta_i(t-\tau)}}\right)-erfc\left(\frac{y_{i+1}^{'}}{\sqrt{2\eta_i(t-\tau)}}\right)\right]d\tau\end{array}\right\} \quad (4.7)$$

Define

$$u = (t-\tau)^{-1/2} \quad \text{and} \quad du = 0.5(t-\tau)^{-3/2} \quad du = 0.5u^3 d\tau \quad (4.8)$$

and consider

$$\int\limits_{t_j}^{t_{j+1}}\frac{\sqrt{\pi\eta_i}}{\sqrt{2}(t-\tau)}\left[erfc\left(\frac{y_i^{'}}{\sqrt{2\eta_i(t-\tau)}}\right)-erfc\left(\frac{y_{i+1}^{'}}{\sqrt{2\eta_i(t-\tau)}}\right)\right]dt'$$

$$= \sqrt{2\pi\eta_i}\int\limits_{(t-t_j)^{-0.5}}^{(t-t_{j+1})^{-0.5}}\frac{1}{u^2}\left[erfc\left(\frac{y_i^{'}u}{\sqrt{2\eta_i}}\right)-erfc\left(\frac{y_{i+1}^{'}u}{\sqrt{2\eta_i}}\right)\right]du \quad (4.9)$$

Because

$$\int\limits_{a}^{b}erfc(cz)z^{-2}dz = \frac{erfc(ca)}{a}-\frac{erfc(cb)}{b}-\frac{2c}{\sqrt{\pi}}\int\limits_{a}^{b}\frac{1}{z}\exp\left(-c^2z^2\right)dz \quad (4.10)$$

51

and ([55], p. 109, [56], p. 228)

$$\frac{2c}{\sqrt{\pi}}\int_a^b \frac{1}{z}\exp\left(-c^2 z^2\right)dz = \frac{c}{\sqrt{\pi}}\int_{c^2 a^2}^{c^2 b^2}\frac{\exp(-u)}{u}du = \frac{c}{\sqrt{\pi}}\left[\int_{c^2 a^2}^{\infty}\frac{\exp(-u)}{u}du - \int_{c^2 b^2}^{\infty}\frac{\exp(-u)}{u}du\right]$$

$$= \frac{c}{\sqrt{\pi}}\left[-Ei\left(-c^2 a^2\right)+Ei\left(-c^2 b^2\right)\right] \tag{4.11}$$

and have;

$$\int_a^b erfc(cz)z^{-2}dz = \frac{erfc(ca)}{a}-\frac{erfc(cb)}{b}+\frac{c}{\sqrt{\pi}}\left[Ei\left(-c^2 a^2\right)-Ei\left(-c^2 b^2\right)\right] \tag{4.12}$$

Thus, Eqn. (4.9) can be written as follows;

$$\int_{t_j}^{t_{j+1}}\frac{\sqrt{\pi\eta_i}}{\sqrt{2(t-\tau)}}\left[erfc\left(\frac{y_i'}{\sqrt{2\eta_i(t-\tau)}}\right)-erfc\left(\frac{y_{i+1}'}{\sqrt{2\eta_i(t-\tau)}}\right)\right]d\tau$$

$$= \sqrt{2\pi\eta_i}\left\{\begin{array}{l}\sqrt{t-t_j}\left[erfc\left(\dfrac{y_i'}{\sqrt{2\eta_i\left(t-t_j\right)}}\right)-erfc\left(\dfrac{y_{i+1}'}{\sqrt{2\eta_i\left(t-t_j\right)}}\right)\right] \\[2em] -\sqrt{t-t_{j+1}}\left[erfc\left(\dfrac{y_i'}{\sqrt{2\eta_i\left(t-t_{j+1}\right)}}\right)-erfc\left(\dfrac{y_{i+1}'}{\sqrt{2\eta_i\left(t-t_{j+1}\right)}}\right)\right] \\[2em] +\dfrac{y_i'}{\sqrt{2\pi\eta_i}}\left[Ei\left(-\dfrac{y_i'^2}{2\eta_i\left(t-t_j\right)}\right)-Ei\left(-\dfrac{y_i'^2}{2\eta_i\left(t-t_{j+1}\right)}\right)\right] \\[2em] -\dfrac{y_{i+1}'}{\sqrt{2\pi\eta_i}}\left[Ei\left(-\dfrac{y_{i+1}'^2}{2\eta_i\left(t-t_j\right)}\right)-Ei\left(-\dfrac{y_{i+1}'^2}{2\eta_i\left(t-t_{j+1}\right)}\right)\right]\end{array}\right\} \tag{4.13}$$

Also, have;

$$\int_{t_j}^{t_{j+1}}\frac{\sqrt{\pi\eta_i}}{\sqrt{t-\tau}}d\tau = 2\sqrt{\pi\eta_i}\left(\sqrt{t-t_j}-\sqrt{t-t_{j+1}}\right) \tag{4.14}$$

Substituting Eqns. (4.13) and (4.14) into Eqn. (4.7) yields;

$$\Delta m(0,t) \approx \frac{1422T\sqrt{\pi\eta_i}}{khx_f}\left\{\begin{array}{l} \displaystyle\sum_{j=0}^{M-1}q(\tilde{t}_j)\left(\sqrt{t-t_j}-\sqrt{t-t_{j+1}}\right)+\sum_{j=0}^{M-1}q(\tilde{t}_j)\lim_{N\to\infty}\sum_{i=0}^{N}\frac{\omega^{(0)}\left(\tilde{y}_i',\tilde{t}_j\right)}{2\sqrt{2}} \\[3mm] \left[\begin{array}{l} \sqrt{t-t_j}\left[erfc\left(\dfrac{y_i'}{\sqrt{2\eta_i\left(t-t_j\right)}}\right)-erfc\left(\dfrac{y_{i+1}'}{\sqrt{2\eta_i\left(t-t_j\right)}}\right)\right] \\[5mm] -\sqrt{t-t_{j+1}}\left[erfc\left(\dfrac{y_i'}{\sqrt{2\eta_i\left(t-t_{j+1}\right)}}\right)-erfc\left(\dfrac{y_{i+1}'}{\sqrt{2\eta_i\left(t-t_{j+1}\right)}}\right)\right] \\[5mm] +\dfrac{y_i'}{\sqrt{2\pi\eta_i}}\left[Ei\left(-\dfrac{y_i'^2}{2\eta_i\left(t-t_j\right)}\right)-Ei\left(-\dfrac{y_i'^2}{2\eta_i\left(t-t_{j+1}\right)}\right)\right] \\[5mm] -\dfrac{y_{i+1}'}{\sqrt{2\pi\eta_i}}\left[Ei\left(-\dfrac{y_{i+1}'^2}{2\eta_i\left(t-t_j\right)}\right)-Ei\left(-\dfrac{y_{i+1}'^2}{2\eta_i\left(t-t_{j+1}\right)}\right)\right] \end{array}\right] \end{array}\right\} \quad (4.15)$$

After expanding and rearranging Eqn. (4.15) as follows:

$$\Delta m(0,t) \approx \frac{1422T\sqrt{\pi\eta_i}}{khx_f} \sum_{j=0}^{M-1} q(\tilde{t}_j) \left\{ \begin{array}{l} \left(\sqrt{t-t_j} - \sqrt{t-t_{j+1}}\right) + \\[4pt] \dfrac{\omega^{(0)}\left(\widetilde{y_0'},\tilde{t}_j\right)}{2\sqrt{2}} \left[\begin{array}{l} \sqrt{t-t_j}\, erfc\left(\dfrac{y_0'}{\sqrt{2\eta_i(t-t_j)}}\right) \\[8pt] -\sqrt{t-t_{j+1}}\, erfc\left(\dfrac{y_0'}{\sqrt{2\eta_i(t-t_{j+1})}}\right) \end{array} \right] \\[16pt] + \dfrac{y_0'\,\omega^{(0)}\left(\widetilde{y_0'},\tilde{t}_j\right)}{\sqrt{2\pi\eta_i}}\dfrac{1}{2\sqrt{2}} \\[8pt] \left[Ei\left(-\dfrac{y_0'^2}{2\eta_i(t-t_j)}\right) - Ei\left(-\dfrac{y_0'^2}{2\eta_i(t-t_{j+1})}\right) \right] \\[8pt] + \lim_{N\to\infty} \sum_{i=0}^{N} \left[\omega^{(0)}\left(\widetilde{y_{i+1}'},\tilde{t}_j\right) - \omega^{(0)}\left(\widetilde{y_i'},\tilde{t}_j\right) \right]\dfrac{1}{2\sqrt{2}} \\[8pt] \left[\begin{array}{l} \sqrt{t-t_j}\, erfc\left(\dfrac{y_{i+1}'}{\sqrt{2\eta_i(t-t_j)}}\right) \\[8pt] -\sqrt{t-t_{j+1}}\, erfc\left(\dfrac{y_{i+1}'}{\sqrt{2\eta_i(t-t_{j+1})}}\right) \end{array} \right] \\[16pt] + \dfrac{y_{i+1}'}{\sqrt{2\pi\eta_i}}\left[\omega^{(0)}\left(\widetilde{y_{i+1}'},\tilde{t}_j\right) - \omega^{(0)}\left(\widetilde{y_i'},\tilde{t}_j\right) \right]\dfrac{1}{2\sqrt{2}} \\[8pt] \left[\begin{array}{l} Ei\left(-\dfrac{y_{i+1}'^2}{2\eta_i(t-t_j)}\right) \\[8pt] -Ei\left(-\dfrac{y_{i+1}'^2}{2\eta_i(t-t_{j+1})}\right) \end{array} \right] \end{array} \right\} \tag{4.16}$$

Eqn. (4.16) can be further simplified by noting that $y_0' = 0$;

$$\Delta m(0,t) \approx \frac{1422T\sqrt{\pi\eta_i}}{khx_f} \sum_{j=0}^{M-1} q(\widetilde{t}_j) \left\{ \begin{array}{l} \left[\left(1 + \frac{\omega^{(0)}\left(\widetilde{y}_0',\widetilde{t}_j\right)}{2\sqrt{2}} \right) \left(\sqrt{t-t_j} - \sqrt{t-t_{j+1}} \right) \right. \\ + \\ \lim_{N\to\infty} \frac{\left[\omega^{(0)}\left(\widetilde{y}_{i+1}',\widetilde{t}_j\right) - \omega^{(0)}\left(\widetilde{y}_i',\widetilde{t}_j\right) \right]}{2\sqrt{2}} \\ \left[\begin{array}{l} \sqrt{t-t_j}\,erfc\left(\frac{y_{i+1}'}{\sqrt{2\eta_i\left(t-t_j\right)}} \right) \\ -\sqrt{t-t_{j+1}}\,erfc\left(\frac{y_{i+1}'}{\sqrt{2\eta_i\left(t-t_{j+1}\right)}} \right) \end{array} \right] \\ + \frac{y_{i+1}'}{\sqrt{2\pi\eta_i}} \left[\begin{array}{l} Ei\left(-\frac{y_{i+1}'^2}{2\eta_i\left(t-t_j\right)} \right) \\ -Ei\left(-\frac{y_{i+1}'^2}{2\eta_i\left(t-t_{j+1}\right)} \right) \end{array} \right] \end{array} \right\} \tag{4.17}$$

where having used;

$$y_0'\,Ei\left(-\frac{y_0'^2}{2\eta_i\left(t-t_j\right)} \right) = 0 \tag{4.18}$$

Eqn. (4.17) is the discretized form of the solution at the fracture plane. However, it still requires the pressures in the entire reservoir (all y_i' for $i=1,2,...,\infty$) to be able to evaluate the $\omega^{(0)}\left(\widetilde{y}_i',\widetilde{t}_j\right)$ terms at every time step. Below, try to find a suitable approximation to alleviate this difficulty.

4.2. Approximate Solution

Here, an approximation is obtained for Eqn. (4.15), which is reasonably accurate for practical applications, by evaluating Eqn. (4.17) asymptotically at short- and long-times. For the geometry considered in this problem, there is only one flow regime (linear flow) for all times and the short- and long-time approximations should yield the same result, which will be taken as the approximate solution.

4.2.1. Short-Term Approximation

Consider Eqn. (4.17) as $t \to 0$. The following assumptions are made;

$$\lim_{t, t_j \to 0} \left[\sqrt{t - t_j} \, erfc \left(\frac{y'}{\sqrt{2\eta_i \left(t - t_j \right)}} \right) \right] = 0 \quad \text{for} \quad y' \neq 0 \tag{4.19}$$

and

$$\lim_{t, t_j \to 0} \left[y' Ei \left(-\frac{y'^2}{2\eta_i \left(t - t_j \right)} \right) \right] = 0 \quad \text{for all } y' \tag{4.20}$$

Then, the following short-term approximation is obtained for Eqn. (4.17);

$$\lim_{t \to 0} \Delta m(0, t) \approx \frac{1422 T \sqrt{\pi \eta_i}}{khx_f} \left[\sum_{j=0}^{M-1} q(\tilde{t}_j) \left(1 + \frac{\omega^{(0)} \left(\tilde{y}_0', \tilde{t}_j \right)}{2\sqrt{2}} \right) \left(\sqrt{t - t_j} - \sqrt{t - t_{j+1}} \right) \right] \tag{4.21}$$

56

4.2.2. Long-Term Approximation

Evaluate the approximate form of Eqn. (4.17) as $t \to \infty$. From Abramowitz and Stegun [56], we have;

$$Ei(-x) = \gamma + \ln|x| - \sum_{n=1}^{\infty} \frac{(-1)^{n-1}}{nn!} x^n \tag{4.22}$$

Then, write;

$$
\frac{y_i'}{\sqrt{\pi \eta_i}} \left[Ei\left(-\frac{y_{i+1}'^2}{2\eta_i (t-t_j)} \right) - Ei\left(-\frac{y_{i+1}'^2}{2\eta_i (t-t_{j+1})} \right) \right]
$$

$$
= \frac{y_i'}{\sqrt{\pi \eta_i}} \left[\ln\left(\frac{t-t_{j+1}}{t-t_j} \right) - \sum_{n=1}^{\infty} \frac{(-1)^{n-1}}{nn!} \left(\frac{y_i'^2}{2\eta_i} \right)^n \frac{\left(\frac{t-t_{j+1}}{t-t_j} \right) - 1}{(t-t_{j+1})^n} \right] \tag{4.23}
$$

Assume that;

$$\lim_{t \to \infty} \frac{t-t_{j+1}}{t-t_j} \approx 1 \tag{4.24}$$

so that

$$\lim_{t \to \infty} \frac{\left(\frac{t-t_{j+1}}{t-t_j} \right) - 1}{(t-t_{j+1})^n} \approx 0 \tag{4.25}$$

and

$$\lim_{t \to \infty} \ln\left(\frac{t - t_{j+1}}{t - t_j}\right) \approx 0 \qquad (4.26)$$

This shows that;

$$\lim_{t \to \infty} \frac{y_i'}{\sqrt{\pi \eta_i}}\left[Ei\left(-\frac{y_{i+1}'^2}{2\eta_i(t - t_j)}\right) - Ei\left(-\frac{y_{i+1}'^2}{2\eta_i(t - t_{j+1})}\right)\right] \approx 0 \qquad (4.27)$$

Therefore, as $t \to \infty$, Eqn. (4.17) is approximated by;

$$\Delta m(0,t) \approx \frac{1422T\sqrt{\pi\eta_i}}{khx_f}\sum_{j=0}^{M-1}q(\tilde{t}_j)\left\{\begin{array}{l}\left(1 + \frac{\omega^{(0)}\left(\widetilde{y_0'},\tilde{t}_j\right)}{2\sqrt{2}}\right)\left(\sqrt{t-t_j} - \sqrt{t-t_{j+1}}\right) \\[2ex] + \\[1ex] \lim_{N \to \infty}\frac{\left[\omega^{(0)}\left(\widetilde{y_{i+1}'},\tilde{t}_j\right) - \omega^{(0)}\left(\widetilde{y_i'},\tilde{t}_j\right)\right]}{2\sqrt{2}} \\[2ex] \left\{\begin{array}{l}\left[\sqrt{t-t_j}\,erfc\left(\frac{y_{i+1}'}{\sqrt{2\eta_i(t-t_j)}}\right)\right. \\[2ex] \left.-\sqrt{t-t_{j+1}}\,erfc\left(\frac{y_{i+1}'}{\sqrt{2\eta_i(t-t_{j+1})}}\right)\right]\end{array}\right\}\end{array}\right\} \qquad (4.28)$$

Further assume that;

$$\lim_{t \to \infty, t_j \neq t}\sqrt{t - t_j}\,erfc\left(\frac{y_i'}{\sqrt{2\eta_i(t - t_j)}}\right) \approx 0 \quad \text{for} \quad y_i' \neq 0 \qquad (4.29)$$

Then, obtain,

$$\lim_{t\to\infty} \Delta m(0,t) \approx \frac{1422T\sqrt{\pi\eta_i}}{khx_f} \left[\sum_{j=0}^{M-1} q(\tilde{t}_j) \left(1 + \frac{\omega^{(0)}\left(\tilde{y}_0^{'},\tilde{t}_j\right)}{2\sqrt{2}} \right) \left(\sqrt{t-t_j} - \sqrt{t-t_{j+1}} \right) \right] \qquad (4.30)$$

which is the same as the short-time approximation given by Eqn. (4.21). Therefore, Eqn. (4.30) can be taken as an appropriate approximation for the fractured tight-gas well solution under strong variability of viscosity and compressibility.

4.2.3. Generalized Approximation for the Perturbation-Green's Function Solution

Consider Eqn. (4.30) as the approximate solution for the fractured tight-gas well solution with variable viscosity and compressibility. Expand Eqn. (4.30) as follows;

$$
\begin{aligned}
\Delta m(0,t) &\approx \frac{1422T\sqrt{\pi\eta_i}}{khx_f} \left[\sum_{j=0}^{M-1} q(\tilde{t}_j) \left(1 + \frac{\omega^{(0)}\left(\tilde{y}_0^{'},\tilde{t}_j\right)}{2\sqrt{2}} \right) \left(\sqrt{t-t_j} - \sqrt{t-t_{j+1}} \right) \right] \\
&= \frac{1422T\sqrt{\pi\eta_i}}{khx_f} \left\{ \begin{array}{l} q(\tilde{t}_0)\sqrt{t} + \sum_{j=1}^{M-1} \left[q(\tilde{t}_j) - q(\widetilde{t_{j-1}}) \right] \sqrt{t-t_j} \\[2mm] -q(\tilde{t}_0)\dfrac{\omega^{(0)}\left(0,\tilde{t}_0\right)}{2\sqrt{2}}\sqrt{t} - \sum_{j=1}^{M-1}\left[q(\tilde{t}_j) - q(\widetilde{t_{j-1}}) \right]\dfrac{\omega^{(0)}\left(0,\tilde{t}_0\right)}{2\sqrt{2}}\sqrt{t-t_j} \end{array} \right\}
\end{aligned}
\qquad (4.31)
$$

Simplifying and rearranging Eqn. (4.31), the approximate solution can be written in the following more familiar form;

$$\Delta m(0,t) = \frac{1422T\sqrt{\pi\eta_i}}{khx_f} \left\{ \begin{array}{l} q(\tilde{t}_0)\left[1 - \dfrac{\omega^{(0)}\left(0,\tilde{t}_0\right)}{2\sqrt{2}} \right]\sqrt{t} \\[4mm] + \sum_{j=1}^{M-1}\left[q(\tilde{t}_j) - q(\widetilde{t_{j-1}}) \right]\left[1 - \dfrac{\omega^{(0)}\left(0,\tilde{t}_j\right)}{2\sqrt{2}} \right]\sqrt{t-t_j} \end{array} \right\} \qquad (4.32)$$

Eqn. (4.32) can be written as;

$$\Delta m(0,t) = \frac{1422T\sqrt{\pi\eta_i}}{khx_f} t_s \tag{4.33}$$

where t_s is the superposition time defined by;

$$t_s = q(\widetilde{t_0})\left[1 - \frac{\omega^{(0)}(0,\widetilde{t_0})}{2\sqrt{2}}\right]\sqrt{t} + \sum_{j=1}^{M-1}\left[q(\widetilde{t_j}) - q(\widetilde{t_{j-1}})\right]\left[1 - \frac{\omega^{(0)}(0,\widetilde{t_j})}{2\sqrt{2}}\right]\sqrt{t-t_j} \tag{4.34}$$

Note that Eqns. (4.32) through (4.34) reduce to the following well-known results, respectively, for 1D linear flow when the variation of viscosity-compressibility product is negligible;

$$\Delta m(0,t) = \frac{1422T\sqrt{\pi\eta_i}}{khx_f}\left\{q(\widetilde{t_0})\sqrt{t} + \sum_{j=1}^{M-1}\left[q(\widetilde{t_j}) - q(\widetilde{t_{j-1}})\right]\sqrt{t-t_j}\right\} \tag{4.35}$$

$$\Delta m(0,t) = \frac{1422T\sqrt{\pi\eta_i}}{khx_f} t_s \tag{4.36}$$

and

$$t_s = \left\{q(\widetilde{t_0})\sqrt{t} + \sum_{j=1}^{M-1}\left[q(\widetilde{t_j}) - q(\widetilde{t_{j-1}})\right]\sqrt{t-t_j}\right\} \tag{4.37}$$

4.3. Verification of the Approximate Solution

The approximated perturbation-Green's function solution (Eqn. (4.32)) leads us to a new superposition time definition (Eqn. (4.34)). This new superposition time, responsible for the large variations in viscosity compressibility due to huge pressure drops at the fracture surface, is derived for infinite, homogeneous, isotropic gas

reservoirs. If we split Eqn. (4.32) into two parts, we can get the 0th ($\Delta m^{(0)}$) and 1st order ($\Delta m^{(1)}$) perturbation solutions. Consequently, it will be obvious to see the difference between constant viscosity-compressibility product solution and the variable one.

$$\Delta m^{(0)}\left(0,t\right)=\frac{1422T\sqrt{\pi\eta_i}}{khx_f}\left\{q(\widetilde{t_0})\sqrt{t}+\sum_{j=1}^{M-1}\left[q(\widetilde{t_j})-q(\widetilde{t_{j-1}})\right]\sqrt{t-t_j}\right\} \tag{4.38}$$

$$\Delta m^{(1)}\left(0,t\right)=-\frac{1422T\sqrt{\pi\eta_i}}{khx_f}\left\{\begin{array}{l}q(\widetilde{t_0})\left[\dfrac{\omega^{(0)}\left(0,\widetilde{t_0}\right)}{2\sqrt{2}}\right]\sqrt{t}\\[4mm]+\sum_{j=1}^{M-1}\left[q(\widetilde{t_j})-q(\widetilde{t_{j-1}})\right]\left[\dfrac{\omega^{(0)}\left(0,\widetilde{t_j}\right)}{2\sqrt{2}}\right]\sqrt{t-t_j}\end{array}\right\} \tag{4.39}$$

For the verification of the approximate perturbation-Green's function solution, the previous synthetic cases mentioned in Chapter 3 was going to be used in order to show the agreement between numerical and analytical solutions of perturbation solution.

4.3.1. Case 1 - Constant bottomhole pressure case

The pseudopressure drops obtained with spectral solution [40], the approximated perturbation-Green's function solution and the numerical solution of the truncated perturbation solution were demonstrated in Figure 4.1. As can be seen from Figure 4.1, after initial flow period approximated perturbation-Green's function solution, numerical solution of the truncated perturbation solution and spectral solution [40] agreed fairly.

Figure 4.1. Pseudopressure drops comparison for spectral solution, analytical and numerical perturbation solutions for Case 1

Figure 4.2 shows the 0th, 1st order perturbation and also the truncated perturbation solutions which were calculated both numerically and analytically. As can be seen from Figure 4.2, the numerical and analytical results are in close agreement. This figure also shows how the change in viscosity and compressibility affect the pseudopressure drop. If we ignore the large variation of viscosity-compressibility product with pressure (leading us $\Delta m^{(0)}$), the calculated pseudopressure drops will deviate from the actual. Therefore, 1st order perturbation term which considers this deviation is added to 0th order perturbation solution.
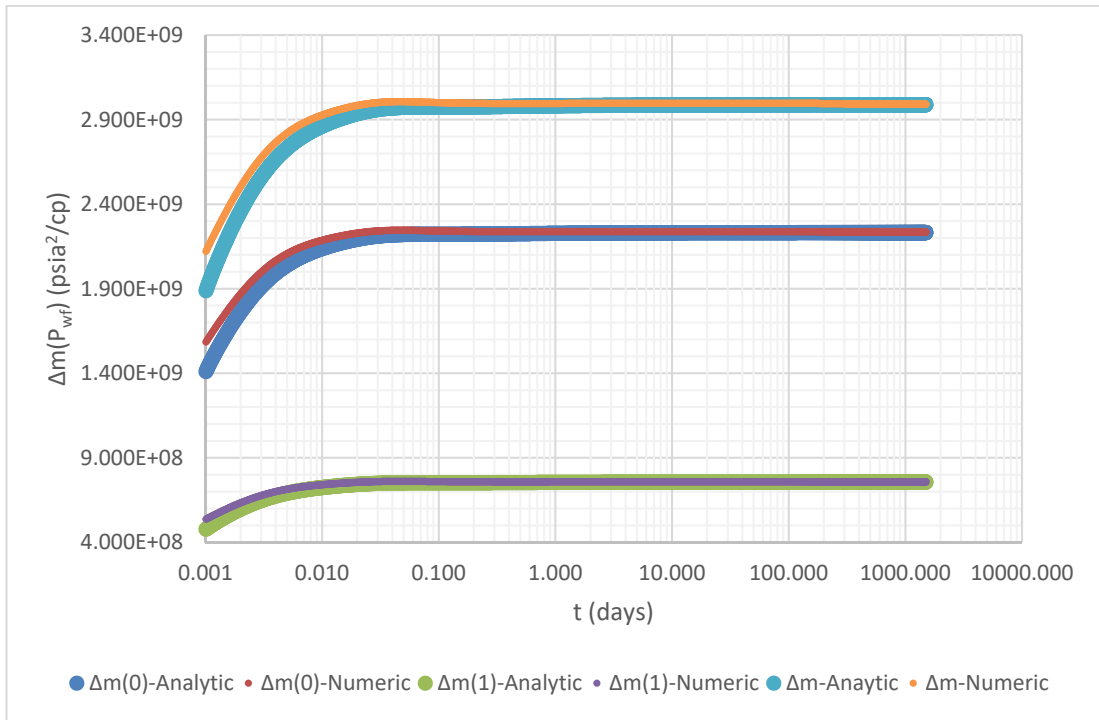
Figure 4.2. 0th and 1st perturbation solutions evaluated both numerically and
analytically for Case 1

4.3.2. Case 2 – Variable bottomhole pressure case

For the variable bottomhole pressure case i.e. Case 2, the pseudopressure drops
obtained from perturbation-Green's function solution, spectral solution [40] and the
numeric solution of truncated perturbation solution are presented in Figure 4.3. The
analytical solution of the truncated perturbation-Green's function solution and
numerical solution of the truncated perturbation solution are in close agreement and
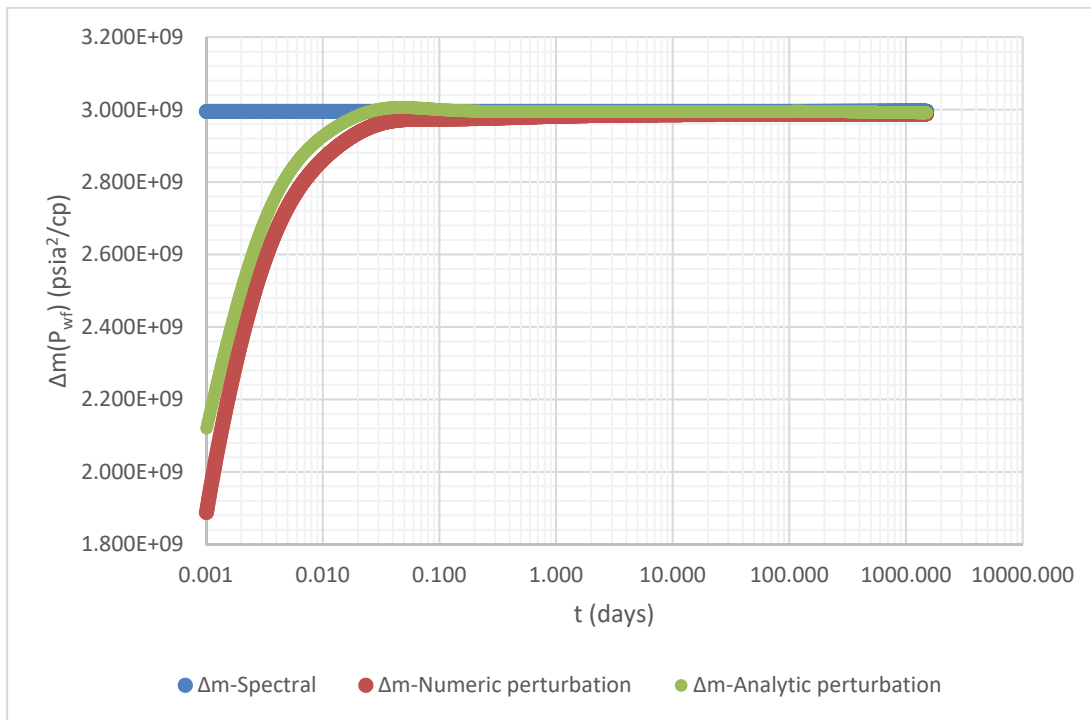they intercept with spectral solution after some time as can be seen from Figure 4.3.

63
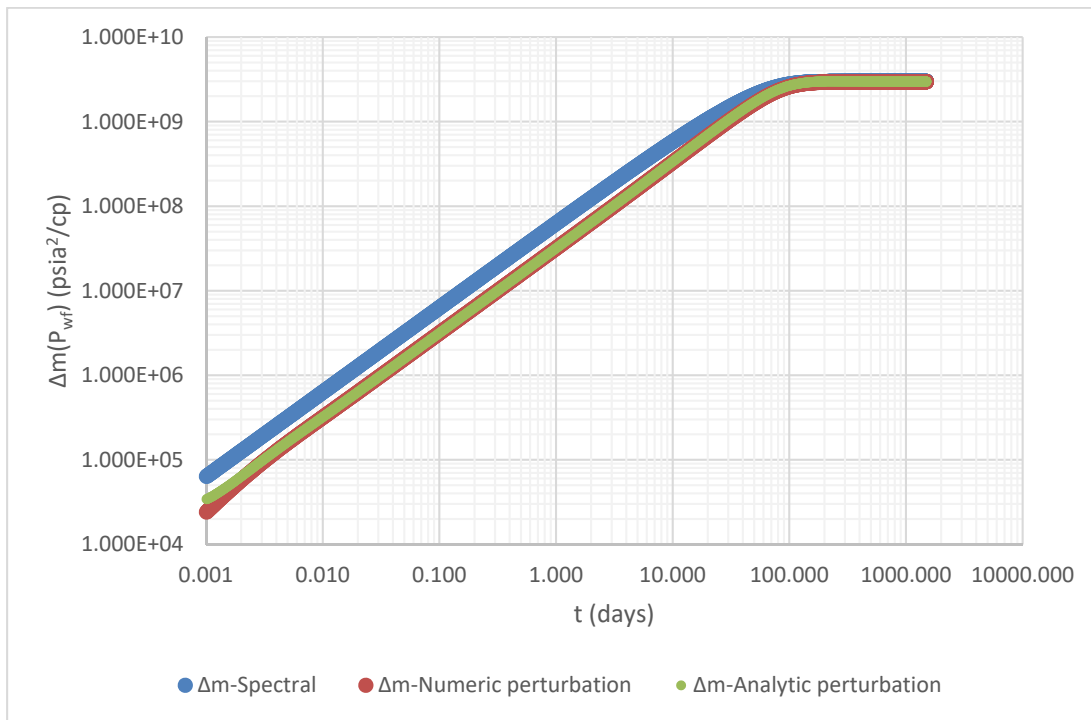
Figure 4.3. Pseudopressure drops comparison for spectral, analytical and numerical perturbation solutions for Case 2

Figure 4.4 shows the $0^{th}, 1^{st}$ order perturbation solutions obtained from analytic and numeric solution of perturbation-Green's function. It is obvious from the Figure 4.4 that analytic and numeric solutions of the perturbation-Green's function solutions for 0th and 1st order perturbation equations are in close agreement. Figure 4.4 presents the difference between constant viscosity-compressibility product solution and the variable viscosity compressibility product solution. When the variation in viscosity compressibility product with pressure is ignored, the corresponding calculated pseudopressure drops $(\Delta m^{(0)}(0,t))$ is actually low compared to variable viscosity compressibility case. Therefore, a correction term $\Delta m^{(1)}(0,t)$ is added to the solution that accounts for the deviation from its initial value.
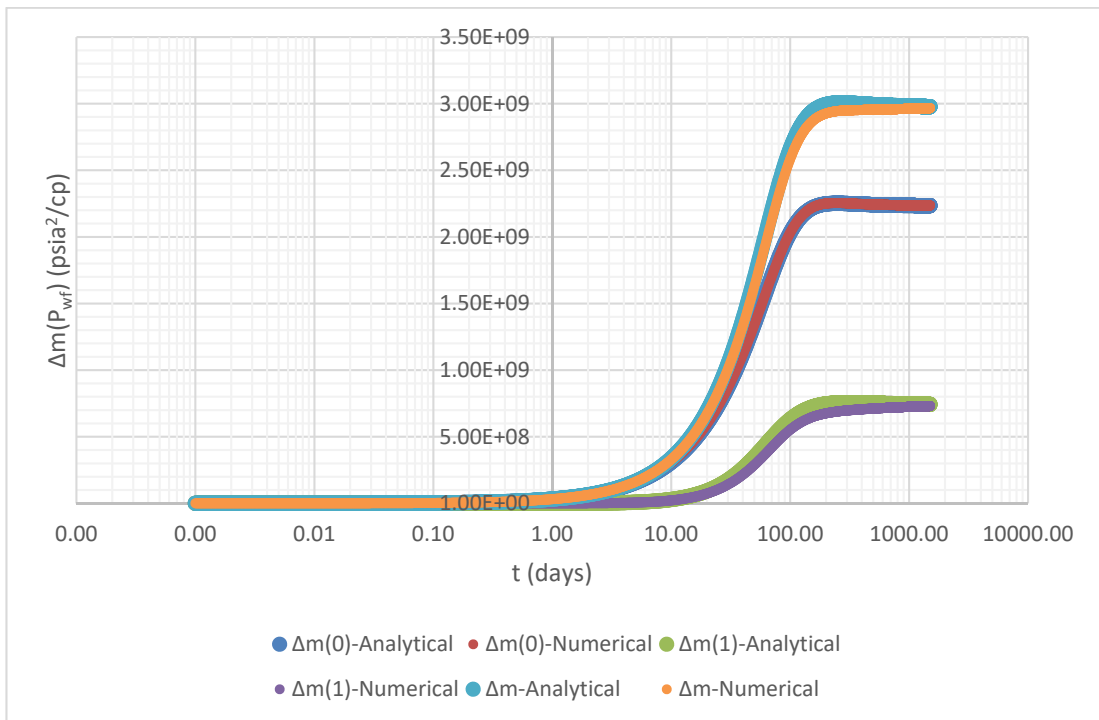
Figure 4.4. 0th and 1st perturbation solutions evaluated both numerically and analytically for Case 2

CHAPTER 5

DISCUSSION OF RESULTS AND EXAMPLE APPLICATIONS

In this chapter, linear flow analysis is going to be performed with rate normalized pseudopressure drop and superposition time. Two previously mentioned synthetic cases (Case 1 and Case 2) and field data are going to be used for the application. Linear flow analysis is going to be carried out with the conventional superposition time and new superposition time. Then, the errors are going to be calculated to show the calculation accuracy in $x_f \sqrt{k}$ for synthetic cases.

For the conventional superposition time analysis, Eqn. (4.40) is used;

$$\Delta m(0,t) = \frac{1422T\sqrt{\pi\eta_i}}{khx_f}\left\{ q(\widetilde{t_0})\sqrt{t} + \sum_{j=1}^{M-1}\left[q(\widetilde{t_j}) - q(\widetilde{t_{j-1}}) \right]\sqrt{t-t_j} \right\} \qquad (4.40)$$

which is actually the 0th order perturbation equation not considering the large variations in viscosity and compressibility.

For the new superposition time analysis, Eqn. (4.41) is used;

$$\Delta m(0,t) = \frac{1422T\sqrt{\pi\eta_i}}{khx_f}\left\{ \begin{array}{l} q(\widetilde{t_0})\left[1 - \dfrac{\omega^{(0)}\left(0,\widetilde{t_0}\right)}{2\sqrt{2}} \right]\sqrt{t} \\[2em] + \sum_{j=1}^{M-1}\left[q(\widetilde{t_j}) - q(\widetilde{t_{j-1}}) \right]\left[1 - \dfrac{\omega^{(0)}\left(0,\widetilde{t_j}\right)}{2\sqrt{2}} \right]\sqrt{t-t_j} \end{array} \right\} \qquad (4.41)$$

which is the approximated perturbation-Green's function equation developed in Chapter 4 taking into account the variations in viscosity and compressibility with pressure.

For rate-normalized pseudopressure drop equation, Eqns. (4.40) and (4.41) can be arranged as respectively, and if we insert η_i into equations, the following equations can be obtained;

$$\frac{\Delta m(0,t)}{q(t)} = \frac{200.5T}{hx_f\sqrt{k\phi\left(\mu_g c_g\right)_i}}\left\{\frac{q(\widetilde{t_0})}{q(t)}\sqrt{t} + \sum_{j=1}^{M-1}\frac{\left[q(\widetilde{t_j})-q(\widetilde{t_{j-1}})\right]}{q(t)}\sqrt{t-t_j}\right\} \qquad (4.42)$$

$$\frac{\Delta m(0,t)}{q(t)} = \frac{200.5T}{hx_f\sqrt{k\phi\left(\mu_g c_g\right)_i}}\left\{\begin{array}{l}\dfrac{q(\widetilde{t_0})}{q(t)}\left[1-\dfrac{\omega^{(0)}\left(0,\widetilde{t_0}\right)}{2\sqrt{2}}\right]\sqrt{t} \\[3mm] +\displaystyle\sum_{j=1}^{M-1}\dfrac{\left[q(\widetilde{t_j})-q(\widetilde{t_{j-1}})\right]}{q(t)}\left[1-\dfrac{\omega^{(0)}\left(0,\widetilde{t_j}\right)}{2\sqrt{2}}\right]\sqrt{t-t_j}\end{array}\right\} \qquad (4.43)$$

Therefore, we can write the conventional superposition time equation coming from Eqn. (4.42) as,

$$t_{\text{sup},con} = \frac{q(\widetilde{t_0})}{q(t)}\sqrt{t} + \sum_{j=1}^{M-1}\frac{q(\widetilde{t_j})-q(\widetilde{t_{j-1}})}{q(t)}\sqrt{t-t_j} \qquad (4.44)$$

and the new superposition time from Eqn. (4.43) as,

$$t_{\text{sup},new} = \frac{q(\widetilde{t_0})}{q(t)}\left[1-\frac{\omega^{(0)}\left(0,\widetilde{t_0}\right)}{2\sqrt{2}}\right]\sqrt{t} + \sum_{j=1}^{M-1}\frac{q(\widetilde{t_j})-q(\widetilde{t_{j-1}})}{q(t)}\left[1-\frac{\omega^{(0)}\left(0,\widetilde{t_j}\right)}{2\sqrt{2}}\right]\sqrt{t-t_j} \qquad (4.45)$$

For Eqns. (4.42) and (4.43), if we plot superposition time versus rate normalized pseudopressure drop, the slope will be equal to;

$$Slope = \frac{200.5T}{h x_f \sqrt{k\phi\left(\mu_g c_g\right)_i}}$$ (4.46)

from which we can get $x_f \sqrt{k}$.

5.1. Case 1 - Constant Bottomhole Pressure Case

For the linear flow analysis the rate normalized pseudopressure drop is plotted against the conventional superposition time and new superposition time in Figure 5.1.

Figure 5.1. Rate normalized pseudopressure drop versus conventional superposition time and new superposition time for Case 1

From the slopes of the straight lines, $x_f \sqrt{k}$ values were calculated by using Eqn. (4.46) and are shown in Table 5.1. In Table 5.1, the input values, the calculated values

from conventional and new superposition time for $x_f \sqrt{k}$ and the errors in $x_f \sqrt{k}$ values from this calculations are listed. It is obvious from Table 5.1 that the conventional superposition time high slope yields relatively high errors in $x_f \sqrt{k}$ values and results in low permeability values. On the other hand, the error calculated from new superposition time is around 1%. Therefore, we can conclude that the use of conventional superposition time in fractured tight gas well performance cause high errors in reservoir property calculations.

Table 5.1. The input and calculated $x_f \sqrt{k}$ values from conventional and new superposition time and the errors for Case 1

Method	Input	Calculated	Error %
Conventional superposition time	$x_f \sqrt{k} = 1.000$	$x_f \sqrt{k} = 0.746$	25.443
New superposition time	$x_f \sqrt{k} = 1.000$	$x_f \sqrt{k} = 0.998$	0.202

5.2. Case 2 - Variable Bottomhole Pressure Case

For the linear flow analysis, the rate normalized pseudopressure drop versus the conventional superposition time and new superposition time is plotted in Figure 5.2 for the variable bottomhole pressure case.
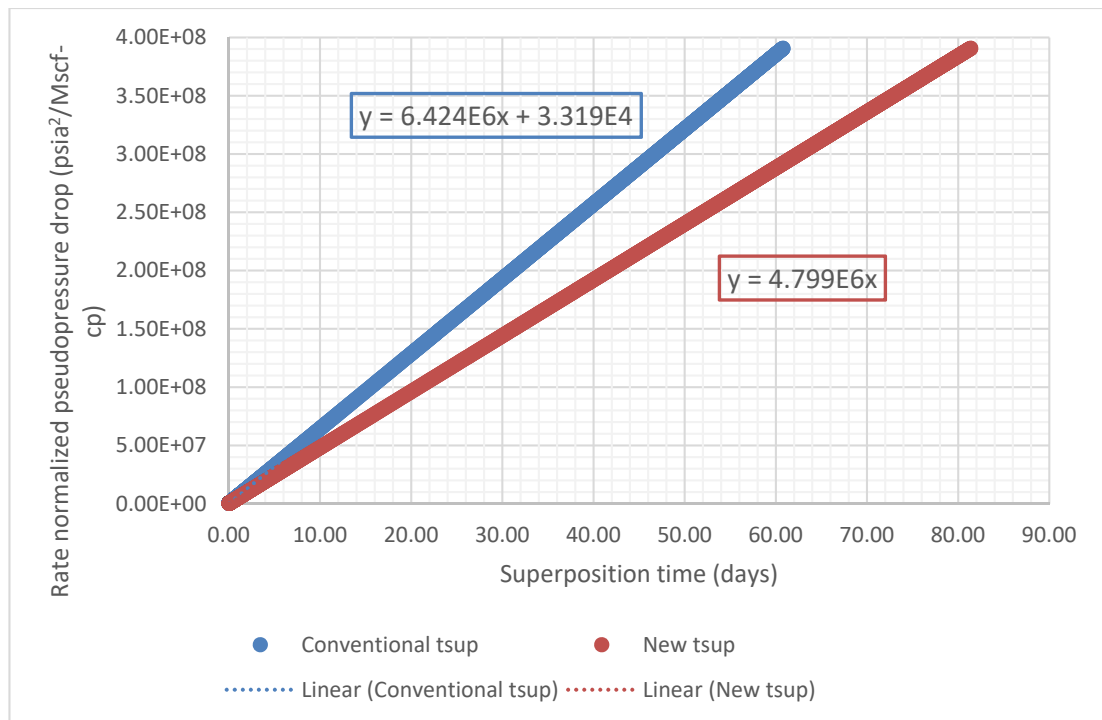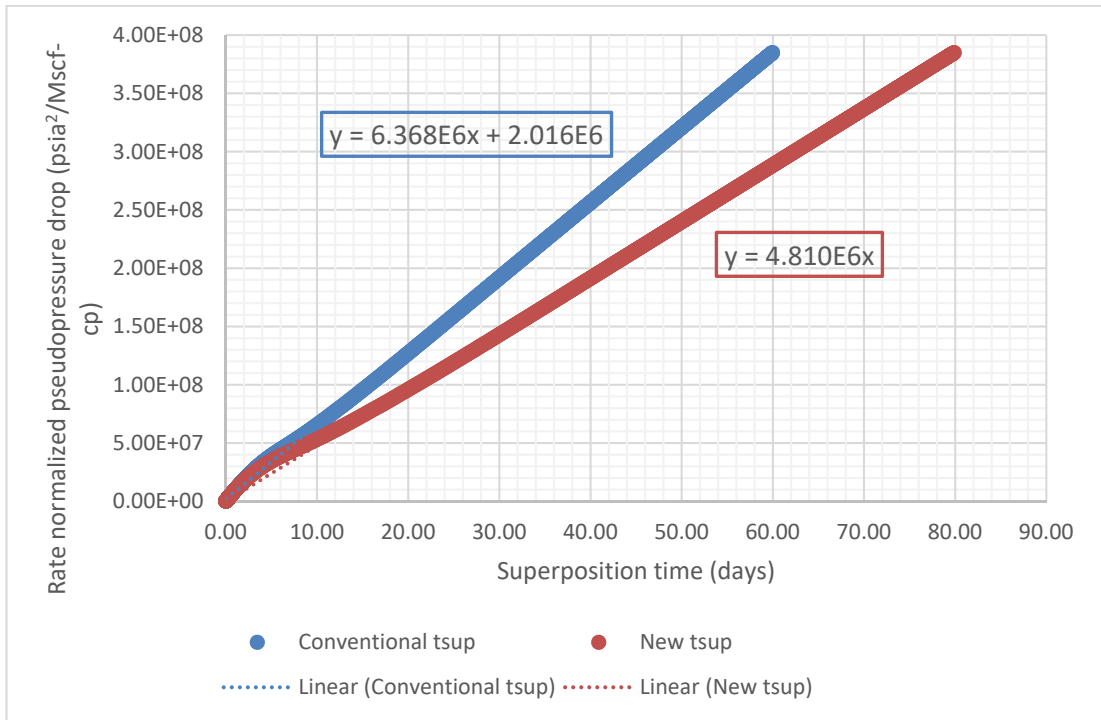
Figure 5.2. Rate normalized pseudopressure drop versus conventional superposition time and new superposition time for Case 2

From the slopes of the straight lines, $x_f \sqrt{k}$ values were calculated from conventional and new superposition time and shown in Table 5.2. In Table 5.2, the input values, the calculated values from conventional and new superposition time and the errors for $x_f \sqrt{k}$ are shown. It can be seen from Table 5.2 that the error calculated from new superposition time is less than 1%.

Table 5.2. The input and calculated $x_f \sqrt{k}$ values from conventional and new superposition time and the errors for Case 2

Method	Input	Calculated	Error %
Conventional superposition time	$x_f \sqrt{k} = 1.000$	$x_f \sqrt{k} = 0.752$	24.787
New superposition time	$x_f \sqrt{k} = 1.000$	$x_f \sqrt{k} = 0.996$	0.429

5.3. Field Case

The new superposition time is also tested in a hydraulically fractured tight gas well data. The reservoir is in infinite-acting flow period; therefore, the flow to the fracture is linear flow. The reservoir rock and fluid properties are given in Table 5.3 for the field.

Table 5.3. Reservoir rock and fluid properties for field case

Matrix permeability, k, mD	0.0011
Matrix porosity, ϕ	0.08
Fracture height, h, ft	260
Initial reservoir pressure, P_i, psia	10400
Reservoir temperature, T, R	707.668
Gas viscosity-compressibility product at initial reservoir pressure, $\left(c_g \mu_g\right)_i$	1.301e-6
Skin, S	0

The wellbore bottomhole pressures and flow rates for the field can be seen in Figure 5.3.
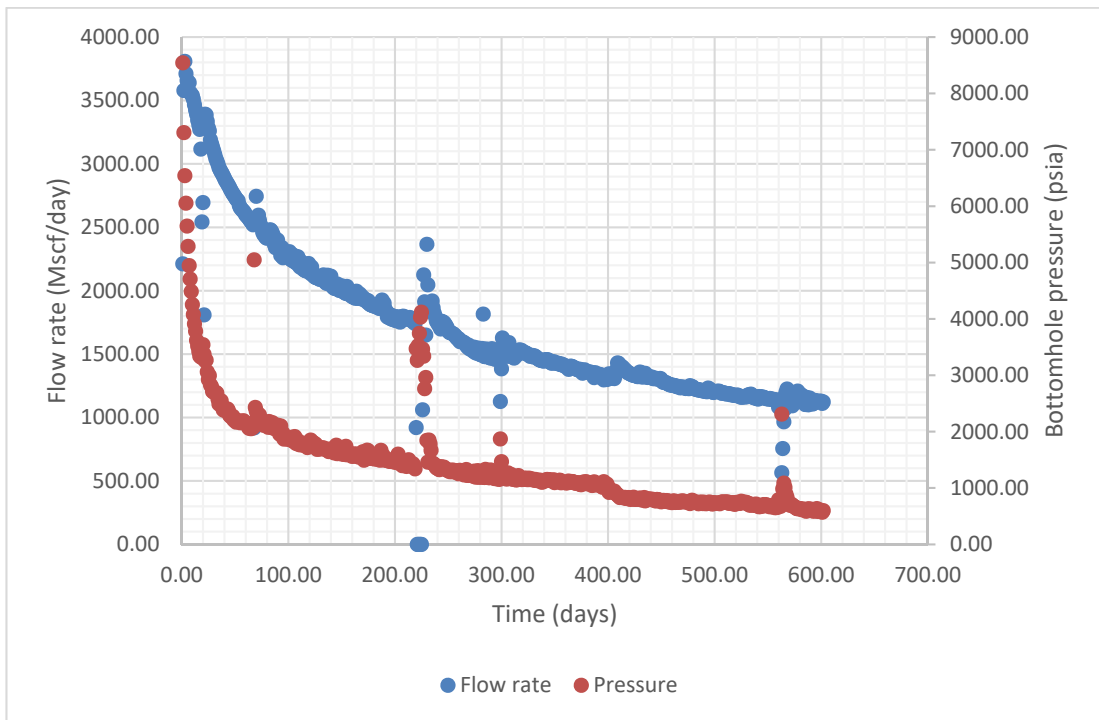
Figure 5.3. Flow rate and bottomhole pressure for a tight gas reservoir

Linear flow analysis is performed by using both the conventional and new superposition time as in the synthetic cases. As can be seen from Figure 5.4, although in the field there is no skin, conventional superposition time plot does not start from origin which indicates skin. The conventional superposition time analysis causes misinterpretation in skin values. The early time distortion of the data from straight line can be due to wellbore storage effect.
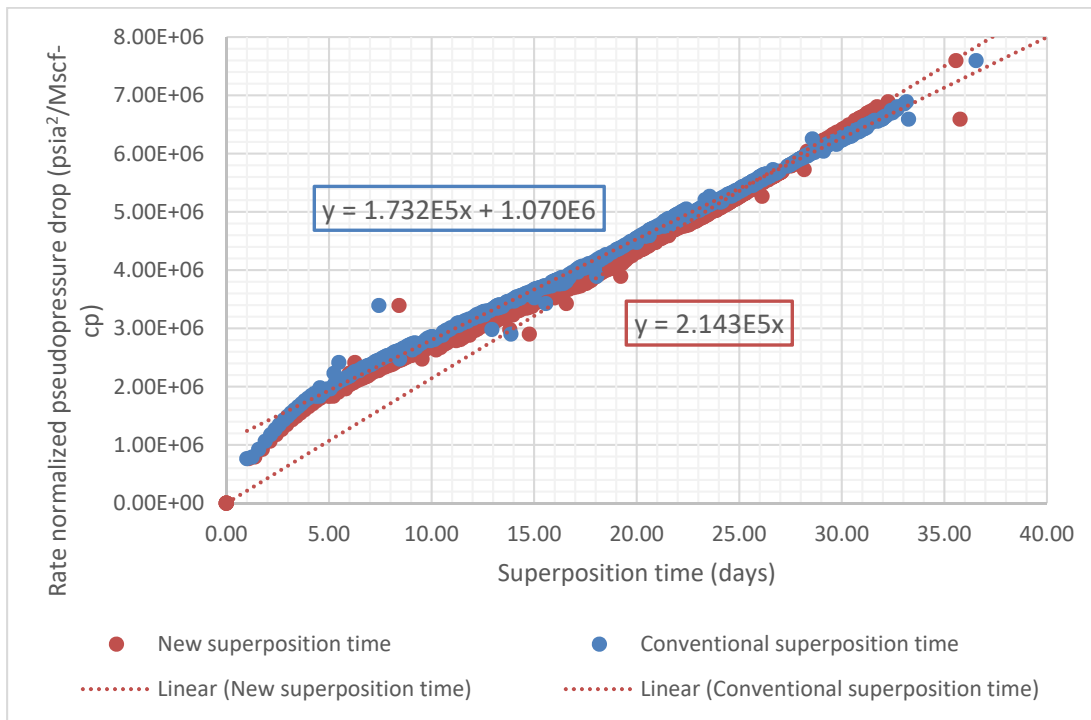
Figure 5.4. Rate normalized pseudopressure versus conventional superposition time and new superposition time for a field data

The $x_f \sqrt{k}$ values calculated from conventional and new superposition time again using Eqn. (4.46) can be seen in Table 5.4.

Table 5.4. The $x_f \sqrt{k}$ values calculated from conventional and new superposition time for a tight gas reservoir

Method	Calculated
Conventional superposition time	$x_f \sqrt{k} = 9.764$
New superposition time	$x_f \sqrt{k} = 7.892$

CHAPTER 6

CONCLUSIONS

In this chapter, the conclusions derived from this study are going to be summarized. In unconventional tight gas reservoirs large pressure gradients are required for production and under these conditions the variation in viscosity-compressibility product is also high. This makes the gas diffusion equation nonlinear. In order to eliminate this nonlinearity, perturbation approach is used. In perturbation method, the nonlinear equation is divided into a series of linear equations and each of them is solved separately which also makes the term-by-term application of superposition principle possible. The main objective of this study is to provide an analytical perturbation-Green's function solution to hydraulically fractured tight gas wells producing under large pressure drops, to investigate the effect of pressure dependent viscosity-compressibility product on the production tight gas well performances and to improve the interpretation from pressure and production data. The solution proposed in this work leads us to a new superposition time which is valid under severe variations in viscosity-compressibility with pressure.

Based on the results of this work, the following conclusions can be outlined;

- An approximated perturbation-Green's function is developed for variable-rate and variable-pressure production data for a fractured tight gas well in an infinite, homogeneous gas reservoir under strong variation in viscosity-compressibility product.
- The approximated perturbation-Green's function numerical and analytical solutions for fractured tight gas well are verified with Thompson's spectral

solution [40] and finite difference simulator, Eclipse. The comparison tests show that the approximated solutions are highly accurate.

- The approximated perturbation-Green's function numerical and analytical solutions present a correction term that considers the deviation of viscosity-compressibility product from its initial value.

- The approximated perturbation-Green's function analytical solution leads us to a practical tool for the analysis of fractured tight gas well performances.

- The approximated perturbation-Green's function analytical solution leads us to a new superposition time equation.

- The estimation of $x_f \sqrt{k}$ values with the use of conventional superposition time is not sufficiently accurate.

- The conventional solution does not take into account the variation in viscosity-compressibility product and this results in misinterpretations in the analysis of tight gas well performances.

- The new superposition time yields highly accurate values in the estimation of $x_f \sqrt{k}$ in synthetic data up to 99%.

CHAPTER 7

RECOMMENDATIONS

The perturbation solution presented in this work is valid for infinite, homogeneous tight gas reservoirs with infinite hydraulic fracture conductivity. More complicated properties can be implemented into the model such as;

- The solution presented in this work is valid for infinite acting reservoir. The solution can be extended to boundary dominated flow conditions.
- There is no skin in this work. The effect of skin can be tested.
- The pressure dependent rock properties like permeability and posrosity can be implemented.
- Klinkenberg effect can be implemented.
- The solution is valid for fully penetrating, infinite conductivity hydraulic fracture. It can be extended to finite conductivity partial penetration case.

REFERENCES

[1] R. Al-Hussainy, H. J. Ramey and P. B. Crawford, "The Flow of Real Gases through Porous Media," *Journal of Petroleum Technology,* vol. 18, no. 5, pp. 624-636, 1965.

[2] A. B. Barreto Jr. and A. M. Peres, "A New Rigorous Analytical Solution for Vertical Fractured Well in Gas Reservoirs," in *SPE Latin American and Caribbean Petroleum Engineering Conference Proceedings*, Mexico City, 2012.

[3] A. B. Barreto Jr., A. M. M. Peres and A. P. Pires, "A Variable-Rate Solution to the Nonlinear Diffusivity Gas Equation by Use of Green's-Function Method," *SPE Journal,* vol. 18, no. 1, pp. 57-68, 2013.

[4] C. Komurcu, "Effect of Viscosity Compressibility Product Variation on the Analysis of Fractured Well Performances in Tight Unconventional Reservoirs," *M. Sc.,* 2014.

[5] M. Ahmadi, "Laplace Transform Deconvolution and Its Application to Perturbation Solution of Non-Linear Diffusivity Equation," *Ph. D.,* 2012.

[6] A. L. Bila, "Application of Superposition in Nonlinear Gas Flow Problems in Porous Media," *M. Sc.,* 2015.

[7] M. A. Schellhardt and E. L. Rawlins, Back-pressure Data on Natural-gas Wells and Their Application to Production Practices, Lord Baltimore Press, 1935.

[8] C. S. Matthews and D. G. Russell, Pressure Buildup and Flow Tests in Wells, Dallas: Society of Petroleum Engineers of AIME, 1967.

[9] K. Aziz, L. Mattar, S. Ko and G. S. Brar, "Use of Pressure, Pressure-Squared or Pseudo-Pressure in the Analysis of Transient Pressure Drawdown Data From Gas Wells," *Journal of Canadian Petroleum Technology,* vol. 15, no. 2, pp. 58-65, 1976.

[10] R. Raghavan, Well Test Analysis, New Jersey: Prentice-Hall, 1993.

[11] R. G. Agarwal, ""Real Gas Pseudo-Time" - A New Function For Pressure Buildup Analysis of MHF Gas Wells," in *SPE Annual Technical Conference and Exhibition*, Nevada, 1979.

[12] J. Finjord, "A Study of Pseudo-Time," *Society of Petroleum Engineers,* 1983.

79

[13] W. J. Lee and S. A. Holditch, "Application of Pseudotime to Buildup Test Analysis of Low-Permeability Gas Wells with Long-Duration Wellbore Storage Distortion," *SPE of AIME,* vol. 34, no. 12, pp. 2877-2887, December 1982.

[14] J. C. Palacio and T. A. Blasingame, "Decline Curve Analysis Using Type Curves - Anaylsis of Gas Well Production Data," *SPE,* 1993.

[15] R. G. Agarwal, D. C. Gardner, S. W. Kleinsteiber and D. D. Fussell, "Analyzing Well Production Data Using Combined-Type-Curve and Decline-Curve Analysis Concepts," *SPE Reservoir Eval. & Eng.,* vol. 50, no. 10, pp. 478-486, October 1999.

[16] M. L. Fraim and R. A. Wattenbarger, "Gas Reservoir Decline Curve Analysis Using Type Curves with Real Gas Pseudo-Pressure and Normalized Time," *SPE Formation Evaluation,* pp. 671-682, December 1987.

[17] D. F. Meunier, C. S. Kabir and M. J. Wittmann, "Gas Well Test Analysis: Use of Normalized Pseudo Variables," *SPE Formation Evaluation,* vol. 2, no. 4, pp. 629-636, December 1987.

[18] M. Ibrahim, R. A. Wattenbarger and W. Helmy, "Determination of OGIP for Wells in Pseudo-Steady State Old Techniques, New Approaches," in *SPE Annual Technical Conference and Exhibition*, Denver, 2003.

[19] A. F. van Everdingen and W. Hurst, "The Application of the Laplace Transformation to Flow Problems in Reservoirs," *Journal of Petroleum Technology,* vol. 1, no. 12, pp. 305-324, 1949.

[20] A. S. Odeh and L. G. Jones, "Pressure Drawdown Analysis, Variable-Rate Case," *Journal of Petroleum Technology,* vol. 17, no. 8, pp. 960-964, August 1965.

[21] M. Y. Soliman, "New Techniques for Analysis of Variable Rate or Slug Test," in *SPE Annual Technical Conference and Exhibition, 4-7 October*, San Antonio, Texas, 1981.

[22] A. F. van Everdingen and L. J. Meyer, "Analysis of Buildup Curves Obtained After Well Treatment," *Journal of Petroleum Technology,* vol. 23, no. 04, pp. 513-524, 1971.

[23] M. J. Fetkovich and M. E. Vienot, "Rate Normalization of Buildup Pressure By Using Afterflow Data," *Journal of Petroleum Technology,* pp. 2211-2224, December 1984.

[24] J. N. Bostic, R. G. Agarwal and R. D. Carter, "Combined Analysis of Postfracturing Performance and Pressure Buildup Data for Evaluating an MHF

Gas Well," *Journal of Petroleum Technology,* vol. 32, no. 10, pp. 1711-1719, 1980.

[25] J. R. Jargon and H. K. van Poollen, "Unit Response Function From Varying-Rate Data," *Journal of Petroleum Technology,* vol. 17, no. 08, pp. 965-969, 1965.

[26] R. G. Agarwal, "A New Method To Account For Producing Time Effects When Drawdown Type Curves Are Used To Analyze Pressure Buildup And Other Test Data," in *SPE Annual Technical Conference and Exhibition, 21-24 September*, Dallas, Texas, 1980.

[27] H. Cinco-Ley and F. Samaniego-V., "Use and Misuse of the Superposition Time Function in Well Test Analysis," in *SPE Annual Technical Conference and Exhibition, 8-11 October*, San Antonio, Texas, 1989.

[28] F. Samaniego-V. and H. Cinco-Ley, "Transient Pressure Analysis for Variable Rate Testing of Gas Wells," in *Low Permeability Reservoirs Symposium, 15-17 April*, Denver, Colorado, 1991.

[29] K. C. Gupta and R. L. Andsager, "Application of Variable Rate Analysis Technique to Gas Wells," in *Fall Meeting of the Society of Petroleum Engineers of AIME, 1-4 October*, New Orleans, Louisiana, 1967.

[30] T. von Schroeter and A. C. Gringarten, "Superposition Principle and Reciprocity for Pressure-Rate Deconvolution of Data From Interfering Wells," in *SPE Annual Technical Conference and Exhibition, 11-14 November, Anaheim*, California, U.S.A., 2007.

[31] R. E. Gladfelter, G. W. Tracy and L. E. Wilsey, "Selecting Wells Which Will Respond to Production-Stimulation Treatment," *American Petroleum Institute,* pp. 117-129, 1955.

[32] H. J. Ramey, "Non-Darcy Flow and Wellbore Storage Effects in Pressure Build-Up and Drawdown of Gas Wells," *Journal of Petroleum Technology,* pp. 223-233, February 1965.

[33] F. J. Kuchuk, "Gladfelter Deconvolution," *SPE Formation Evaluation,* pp. 285-292, September 1990.

[34] A. G. Winestock and G. P. Colpitts, "Advances in Estimating Gas Well Deliverability," *The Journal of Canadian Petroleum,* pp. 111-119, 1965.

[35] D. Meunier, M. J. Wittmann and G. Stewart, "Interpretation of Pressure Buildup Testing Using In-Situ Measurement of Afterflow," *Journal of Petroleum Technology,* pp. 143-152, January 1985.

[36] F. Kuchuk and L. Ayestaran, "Analysis of Simultaneously Measured Pressure and Sandface Flow Rate in Transient Well Testing," *Journal of Petroleum Technology,* pp. 323-334, February 1985.

[37] E. Pimonov, C. Ayan, M. Onur and F. Kuchuk, "A New Pressure/Rate-Deconvolution Algorithm to Analyze Wireline-Formation-Tester and Well-Test Data," *SPE Reservoir Evaluation & Engineering,* pp. 603-613, August 2010.

[38] L. G. Thompson and A. C. Reynolds, "Analysis of Variable-Rate Well-Test Pressure Data Using Duhamel's Principle," *SPE Formation Evaluation,* pp. 453-469, October 1986.

[39] Schlumberger, Eclipse Reservoir Engineering Software, Version 2015.2, 2017.

[40] L. Thompson, "Spectral Solution Code for Tight Gas Flow Analysis," *Personal Communication,* 2014.

[41] T. P. Singh, "An Improved Finite Difference Method for Well Models in Numerical Reservoir Simulation," in *International Conference on Current Trends in Technology*, Ahmedabad, 2011.

[42] N. Kasiri and A. Bashiri, "Comparative Study of Different Techniques for Numerical Reservoir Simulation," *Petroleum Science and Technology,* vol. 28, no. 5, pp. 494-503, 2010.

[43] M. Liu and G. Zhao, "Boundary Element Technique in Petroleum Reservoir Simulation," in *COMSOL Conference*, Boston, 2011.

[44] J. Kikani, Application of Boundary Element Method to Steamline Generation and Pressure Transient Testing, Stanford University, 1989.

[45] L. Thompson, "Characterization of Flow in Fractured Tight Gas Reservoirs," *Personal Communication,* 2012.

[46] D. Kale and L. Mattar, "Solution of a Non-Linear Gas Flow Equation by the Perturbation Technique," *Journal of Canadian Petroleum Technology,* vol. 19, no. 4, pp. 63-67, 1980.

[47] A. M. Peres, K. V. Serra and A. C. Reynolds, "Toward a Unified Theory of Well Testing for Nonlinear-Radial-Flow Problems With Application to Interference Tests," *SPE Formation Evaluation,* vol. 5, no. 2, pp. 151-160, 1990.

[48] A. M. Peres, K. V. Serra and A. C. Reynolds, "Supplement to SPE 18113, Toward a Unified Theory of Well Testing for Nonlinear-Radial-Flow Problems With Application to Interference Tests," *SPE Formation Evaluation,* vol. 5, no. 2, pp. 1-26, 1989.

[49] H. S. Carslaw and J. C. Jaeger, Conduction of Heat in Solids, London: Oxford University Press, 1959.

[50] A. C. Gringarten, H. J. Ramey and R. Raghavan, "Unsteady-State Pressure Distributions Created by a Well with a Single Infinite-Conductivity Vertical Fracture," *Society of Petroleum Engineers Journal,* vol. 14, no. 4, pp. 347-360, 1974.

[51] MATLAB 2017a, The Mathworks, Inc., Natick, Massachusetts, United States.

[52] R. P. Sutton, "Fundamental PVT Calculations for Associated and Gas/Condensate Natural Gas Systems," in *SPE Annual Technical Conference and Exhibition*, Dallas, 2005.

[53] N. Azizi, R. Behbahani and M. A. Isazadeh, "An Efficient Correlation for Calculating Compressibility Factor of Natural Gases," *Journal of Natural Gas Chemistry,* vol. 19, no. 6, pp. 642-645, 2010.

[54] A. L. Lee, M. H. Gonzalez and B. E. Eakin, "The viscosity of natural gases," *Journal of Petroleum Technology,* vol. 18, no. 8, pp. 997-1000, 1966.

[55] I. S. Gradshteyn and I. M. Ryzhik, Tables of Integral Series, and Products, 2007: Academic Press, London.

[56] M. Abramowitz and I. A. Stegun, Handbook of Mathematical Functions With Formulas, Graphs and Mathematical Tables, National Bureau of Standards Applied Mathematics Series, 1965.

CURRICULUM VITAE

Name:	Gül Ertunç, Kıymet Gizem
Born:	Ankara, Turkey
E-mail:	gul.gizemmm@gmail.com
Phone:	+90 312 210 7316
Education:	Middle East Technical University, Ankara, Turkey Master of Science Degree in Petroleum Engineering, 2011
	Middle East Technical University, Ankara, Turkey Bachelor of Science Degree in Petroleum Engineering, 2009
	Middle East Technical University, Ankara, Turkey Minor Degree in Geographical Information Systems, 2009
Work Experience:	Middle East Technical University, Ankara, Turkey Research Assistant, 2009-2017
Publications:	Combustion Characteristics and Kinetic Analysis of Turkish Crude Oils and Their SARA Fractions, Journal of Thermal Analysis and Calorimetry, Vol. 114, October 2013, 269-275.
	Thermal Characteristics and Kinetics of Crude Oils and SARA Fractions, Thermochimica Acta, Vol. 569, October 2013, 66-70.